UNIVERSITY OF OKLAHOMA

GRADUATE COLLEGE

DETERMINING CONFORMATIONAL CHANGE WITHIN THE *ESCHERICHIA COLI* OUTER MEMBRANE PROTEIN FEPA

A DISSERTATION

SUBMITTED TO THE GRADUATE FACULTY

in partial fulfillment of the requirements for the

Degree of

DOCTOR OF PHILOSOPHY

By

VY H. TRINH
Norman, Oklahoma
2013

DETERMINING CONFORMATIONAL CHANGE WITHIN THE *ESCHERICHIA COLI* OUTER MEMBRANE PROTEIN FEPA

A DISSERTATION APPROVED FOR THE
DEPARTMENT OF CHEMISTRY AND BIOCHEMISTRY

BY

_____
Dr. Michael T. Ashby, Chair

_____
Dr. Phillip E. Klebba

_____
Dr. David P. Nagle

_____
Dr. Ann H. West

_____
Dr. Wai Tak Yip

_____
Dr. Elena I. Zgurskaya

Acknowledgements

“Whether or not you can never become great at something, you can always become better at it.” –Neil deGrasse Tyson

I would like to acknowledge my advisor Dr. Phillip “Klebbman” Klebba for helping me become a better researcher. He was a great mentor and supported me when I needed it the most. As the saying goes, behind every great man there’s a great woman and that woman is Dr. Sally Newton. Her research, guidance, and baked goods were greatly appreciated. This perfect duo provided a nurturing atmosphere and a wealth of knowledge. I am grateful for everything they have done for me.

I would also like to thank my current and former committee members: Dr. Ashby, Dr. Cook, Dr. Nagle, Dr. West, Dr. Yip, and Dr. Zgurskaya. Their advice and insight helped in developing my research. I would like to express my gratitude to Dr. Paul Sims and everyone who worked in his lab. Dr. Sims was like a mentor in Dr. Klebba’s absence and I couldn’t be luckier to have worked with both. I would also like to thank the Department of Chemistry and Biochemistry.

I owe special acknowledgements to Dr. Chuck Smallwood, he suggested I join the Klebba lab and because of this I am indebted to him. All of the previous and current lab members have provided great conversation that made coming into lab a pleasure. Lynn, Amparo, and Dr.Kyle Moore were a few people who could calm me down with a

soothing Spanish phrase that I could never say myself but I will never forget it.

I am also thankful to all of my friends outside of the Klebba lab; they had to hear my complaints and witness my paranoia. Dr. Nathan Green entered the program with me and I am happy to say we're still friends at the end.

I would like to thank my friends and family for their support and welcomed distractions during my time in graduate school. I could not ask for better. Finally, I would like to thank James. To quote Homer Simpson, "I just try and make the day not hurt until I can crawl back in with you."

Table of Contents

List of Tables

List of Figures

Abstract

Bacteria have been able to circumvent antibiotic treatment in several ways, e.g., reorganization of the membrane and its permeability, decrease porin content, over expression of efflux pumps, and genetic changes in target sites (1-3). Most aerobic and facultative anaerobic microorganisms synthesize at least one siderophore, which chelates iron, making iron transport systems an appealing target in determining new methods of pathogenic preventions.

Ferric enterobactin (FeEnt) is the native siderophore of *Escherichia coli* (*E. coli*). The mechanism of FeEnt transport through the outer membrane (OM) receptor protein, FepA, is still unknown. FepA is a ligand-gated porin with a globular N-domain occluding the 22-stranded β-barrel C-domain. The occlusion of the ligand-gated porin makes it necessary for conformational change within the N-domain of FepA during FeEnt transport. Two models have been proposed: the ball-and-chain model and the transient pore model; in the former the N-domain is completely expelled into the periplasmic space and the latter requires a structural rearrangement within the β-barrel of FepA.

TonB is essential for transporting all metal complexes through the OM, including FeEnt. The role of TonB is unknown and the concentration of TonB proteins and TonB-dependent receptor proteins is disproportionate. This suggests that there are two populations of TonB-dependent receptor proteins: active transporters associated with TonB

and inactive transporters unassociated with TonB. This discrepancy in protein concentration between the OM transport protein and TonB may explain the slow turnover rate of FeEnt through FepA. The slow turnover rate may also be a result of an intrinsically slow transport mechanism across the OM. Existing radioisotopic assays measure the transport of FeEnt through the passage of the inner membrane (IM), as the accumulation of the iron complex in the cytoplasm. We devised a new assay to observe FeEnt transport through the OM.

The novel post-uptake binding (PUB) determinations provided information on the mechanism of FeEnt transport through FepA. It revealed that all of the FepA proteins were functionally active and could transport FeEnt through the OM. It is possible that the interaction between FepA and TonB is the rate-limiting step, which may explain the low turnover number. PUB determinations from strains lacking FepB or a complete FepCDG inner membrane complex suggested that these proteins were necessary for FeEnt transport through the OM. After determining the FepA proteins were actively transporting FeEnt in the *ΔfepB* strain, it was determined that FeEnt was not retained in the cell. Accumulation of the ligand in the cytoplasm was impaired in strains lacking the periplasmic binding protein or a complete inner membrane FepCDG complex. Retention experiments and PUB determinations revealed TolC exported FeEnt out of the cell.

Kinetic data suggested that ligand uptake through FepA is triphasic with the initial rate being the most rapid, the second rate has an intermediate rate, and the last rate is the slowest. These results have not been previously observed and it may reflect the mechanistic connections to TonB-ExbBD, FepB and FepCDG-Fes. We determined the activation energy of FeEnt internalization through the OM was approximately 35 kcal/mol. The results indicated that the transport of FeEnt through FepA may involve significant conformational changes. These studies have resulted in a publication, Newton, S. M., Trinh, V., Pi, H., and Klebba, P. E. (2010) *J Biol Chem* **285**, 17488-17497.

After determining that all FepA proteins bound to FeEnt actively transport FeEnt, we tried to determine the mechanism of FeEnt transport through FepA using FRET analyses. We engineered several double Cys substituted mutants in FepA. These FepA derivatives were labeled with the donor dye, fluorescein maleimide (FM), and the acceptor dye, Alexa Fluor 546 maleimide (A546M). The fluorescence intensities from an emission scan with an excitation at 488 nm was used to determine if energy transfer was occurring between the two dyes. Using the energy transfer efficiency, the distance between the two dyes could be calculated. Comparing the distance between the dyes in the absence and presence of FeEnt transport through FepA would help determine the mechanism of ligand transport through FepA.

After determining the double Cys mutant derivatives of FepA transported FeEnt similar to wild-type FepA, we optimized fluorescent labeling conditions with FM and A546M. Then, we ran excitation and emission scans of the single and double Cys substituted mutants in FepA. We were unable to show reproducible results that indicated energy transfer between the dyes in the absence or presence of FeEnt transport through FepA.

It was possible that the dipole orientation of the dyes are more static than anticipated, this would result in poor energy transfer between the fluors. By engineering new double Cys substituted mutants in FepA, it should be possible to remedy this problem. The labeling efficiency of A546M may also contribute to the results that indicated energy transfer did not occur between the dyes. If fractional labeling of A546M occurred, it was possible that FepA could be labeled with two FM dyes rather than just one. If the fractional labeling of A546M was determined, it would be possible to adjust the values obtained in the emission scan and determine the distance between the fluors. If we determined the energy transfer between the dyes in the absence and presence of FeEnt transport through FepA, we would determine the mechanism of FeEnt transport through FepA: ball-and-chain or transient pore model.

After determining FRET analysis could not be used for studies involving the conformational change of FepA during FeEnt transport, disulfide bond formation studies were conducted to determine the

conformational change of the N-domain of FepA during FeEnt transport through FepA. We constructed two classes of double Cys mutants in FepA: N-terminus to N-terminus mutants in FepA and N-terminus to C-terminus mutants in FepA.

Siderophore nutrition tests, FeEnt accumulation determinations, and mobility shift assays were conducted under oxidizing and reducing conditions. The first two assays were used to determine if the formation of a disulfide bond hindered the transport of FeEnt through FepA. The N-terminus to N-terminus Cys substituted mutants in FepA were designed so the Cys residues were within cross-linking distance. With the exception of L125C/V141C, all N-terminus to N-terminus mutants in FepA indicated a formation of a disulfide bond within the globular N-domain of FepA. This cross-link hindered FeEnt accumulation through FepA. These results suggested that the N-domain of FepA needed to undergo conformational changes during FeEnt uptake through the OM.

N-terminus to C-terminus mutants were engineered where the Cys residues could not form a disulfide bond in the native FepA or in the absence of FeEnt transport. If the N-domain of FepA was displaced into the periplasmic space, like the ball-and-chain model, it was possible that the Cys residue in the N-domain could come in proximity of the Cys residue in the C-domain and form a disulfide bond. Based on the FeEnt accumulation assays and the siderophore nutrition tests a cross-link did not form between the two Cys substituted residues in FepA. If a disulfide

bond formed, it did not hinder FeEnt transport through FepA. The electrophoretic mobility results indicated that all of the double Cys mutants in FepA formed a disulfide cross-link. This result was just qualitative and there were no quantitative results to determine the effects of the disulfide bond during FeEnt binding or transport.

List of Abbreviations

A546M, Alexa Fluore 546 maleimide
ATP, adenosine triphosphate
βME or βMSH, β-mercaptoethanol
CCCP, carbonyl cyanide m-chlorophenyl hydrazine
ColB, colicin B
CuP, copper/1,10-phenanthroline
DL, double labeled with fluorescein maleimide and Alexa Fluor 546 maliemide
DTT, dithiothreitol
E, energy transfer efficiency
E. coli, *Escherichia coli*
E_a, activation energy
EDTA, ethylenediaminetetraacetic acid
Fc, ferrichrome
FeEnt, ferric enterobactin
FepA, ferric enterobactin porin A
FM, fluorescein maleimide
FRET, Förster resonance energy transfer
Fur, ferric uptake regulator
lgG, immunoglobulin G
IM, inner membrane
LB, Luria-Bertani media
LGP, ligand-gated porin
mAb, monoclonal antibody
MOPS, 3-(N-morpholino)propanesulfonic acid
NEM, N-ethylmaleimide
OM, outer membrane
p23, pITS23
p47, pITS47
PAA, protein A-agarose
PAGE, polyacrylamide gel electrophoresis
R_0, Förster distance
SDS, sodium dodecyl sulfate
SOC, super optimal broth with catabolite repression
TBS, Tris-buffered saline

Chapter 1: Introduction

Iron and Bacteria

Iron is essential for several biosynthetic and metabolic systems within prokaryotes and eukaryotes. Iron is involved in DNA synthesis, electron transport, protection against oxidative stress, and the tricarboxylic acid cycle (4-7). During bacterial infection, iron must be acquired from the host animal for the growth of the pathogen to occur. In mammalian hosts, proteins like lactoferrin and transferrin sequester iron and are a form of defense by limiting iron availability (8). In addition, the concentration of free iron in aerobic conditions is too low (10^{-18} M (9)) for optimal growth of microbes (10^{-8} M to 10^{-6} M (10)). Many bacterial pathogens respond to these iron-limited conditions by developing additional methods to obtain iron: synthesizing iron chelators, known as siderophores; and high affinity iron transport systems and development of receptors that can bind transferrin, lactoferrin, or hemoglobin as a source of iron (11,12).

Siderophores

Siderophores are low molecular weight organic molecules that chelate iron and are secreted under iron-deficient conditions (13). The synthesis of siderophores and their transport systems is regulated by a ferric uptake regulator (Fur) protein or Fur-like proteins (14). Siderophores can be classified by the moieties donating the oxygen ligands for Fe^{3+}: catecholates, hydroxamates, or (α-hydroxy-) carboxylates (15).

Enterobactin is the native siderophore of *E. coli* (16,17). The triscatecholate siderophore is the strongest iron chelating compound ever discovered and can strip iron from ferritin (18,19). Once enterobactin binds iron, it is called ferric enterobactin (FeEnt) and has a negative charge (-3) and is ~700 Da.

Ligand-Gated Porins

In order to internalize iron into the cytoplasm of Gram-negative bacteria, iron must pass through the outer membrane (OM) and inner membrane (IM) bilayers. The OM contains phospholipids, lipopolysaccharides, and proteins, such as the porins OmpF and OmpC. These porins contribute to the membrane permeability with a size exclusion limit of 650 Da (20).

Siderophore complexes are usually larger than 650 Da; therefore, specific receptors transport the metal complexes. These siderophore receptors belong to the class of porins called ligand-gated porins (LGP) (21) and are commonly named after the ligands they transport. Once the LGP is bound to a siderophore, conformational changes activate siderophore internalization through the OM. These ligand-gated porins accumulate the metal against a concentration gradient, which requires energy and the TonB-ExbB-ExbD complex in the IM. Iron siderophore and vitamin B_{12} receptors share similar structure and function, for example FepA, BtuB, FecA and FhuA. FepA, ferric enterobactin porin A, transports FeEnt and similarly to its OM receptor homologues contains a C-terminus

that forms a porin channel consisting of 22 antiparallel β-strands, large extracellular surface loops, and an N-terminus with 150 residues (22). These residues of the N-domain form a globular domain inside the pore. In addition to siderophores, most LGP recognize and interact with colicins and bacteriophages.

FeEnt Uptake

FeEnt uptake through the OM protein FepA is not fully understood. FepA binds a single FeEnt molecule with high affinity (K_d = 0.2 nM (23)) and the binding of FeEnt to FepA exhibits biphasic kinetics (24,25). The initial step is rapid, during which FeEnt is likely bound to the surface loops of FepA primarily by hydrophobic bonds and aromatic residues(26). Previous research suggests that the second binding site consists of aromatic and basic amino acids and is located above apex of the N-domain of FepA (27). These interactions are reasonable considering FeEnt has a negative net charge (-3). This is followed by a slower step which involves the internalization of the ligand.

Once FeEnt passes through the OM, the ferric complex is then bound by the periplasmic protein, FepB (28,29). FepB shuttles FeEnt to the inner membrane complex, FepCDG, which is an ATP-dependent ABC transporter (30,31). Once FeEnt is in the cytoplasm, it is hydrolyzed by an esterase releasing iron to be utilized for cell metabolism (32). An essential component for FeEnt transport is the inner membrane protein TonB and

ExbBD and a source of energy. The initial interaction between FeEnt and FepA is independent of both TonB and an energy source (Fig. 1).

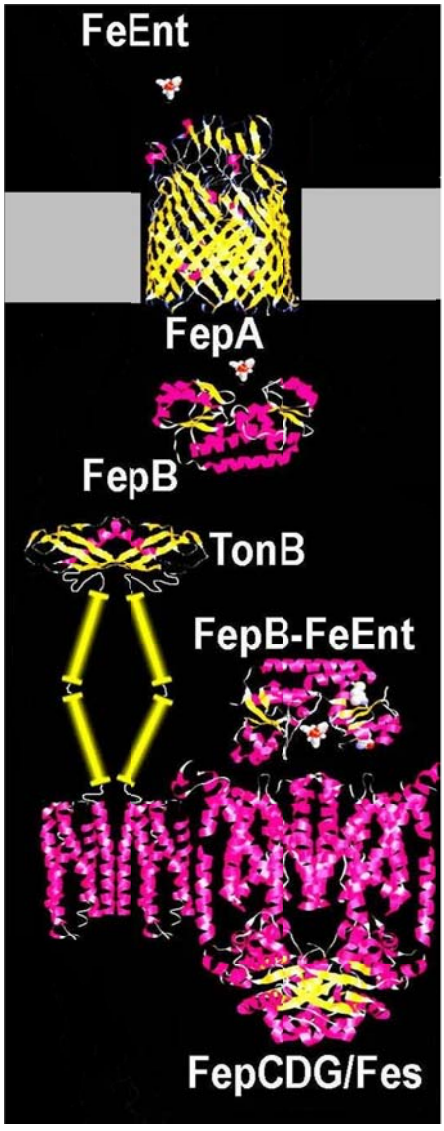

Figure 1. Graphical representation of the FeEnt transport system. FeEnt is bound to the outer membrane protein FepA. Once it passes through the OM (gray bars), the iron complex is bound by FepB, which shuttles FeEnt to the inner membrane complex FepCDG. TonB is essential for FeEnt transport through FepA. Figure adapted from Klebba, P.E. (33)

FeEnt transport through FepA is an active transport and requires energy to internalize the ligand. The porin channels in the OM, make it impossible to maintain an electrochemical potential. In addition, the periplasmic space contains no known energy source (34). The proton motive force of the inner membrane could be the driving force for FeEnt internalization (35).

Because of the necessity for TonB and energy during FeEnt transport through FepA, it has been proposed that TonB functions as an energy transducer for the OM metal receptors and ExbB and ExbD stabilize TonB (34). But this has never been proven and the function of TonB still remains unknown. In FhuA, once ferrichrome binds to the OM receptor, a short β-strand known as the TonB-box relocates, signaling TonB (36).

FepA is a 724 residue protein and contains only 2 cysteines, C487 and C494, which form a disulfide bond together. As mentioned earlier, contains a C-domain β-barrel with the globular N-domain residing within the β-barrel (Fig. 2). The N-domain of FepA is a four-stranded β-sheet with a short 7 residue sequence called the TonB-box which may mediate signal transduction to TonB (37). The N-domain of FepA completely occludes the transmembrane channel and the mechanism of FeEnt transport through FepA is unknown. During FeEnt internalization through FepA, the N-domain of FepA must undergo a structural rearrangement to allow a

passage way for FeEnt. Two possible models have been proposed to describe the ligand transport through FepA (Fig. 3).

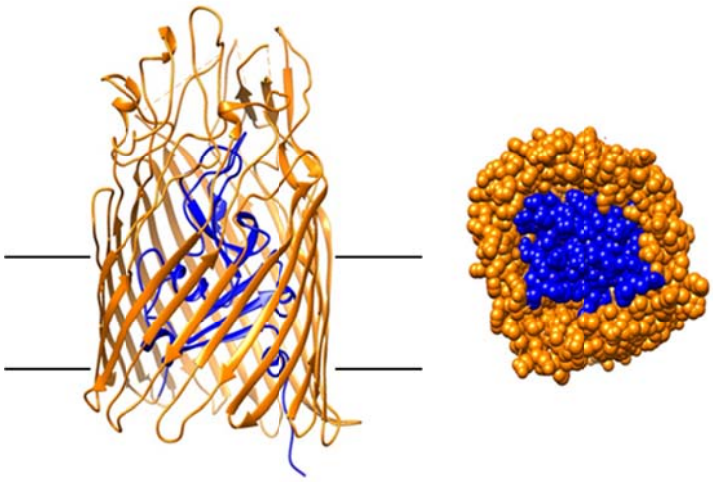

Figure 2. Graphical representation of FepA. To the **left** is a ribbon diagram of FepA. The membrane bilayer is represented by black horizontal lines. The extracellular space is located above the membrane bilayer on top of the figure. The periplasmic space is below the membrane bilayer beneath the figure. The globular N-domain (blue) resides within the β-barrel C-domain (orange) of FepA. To the **right** is a view of FepA from the periplasm, shown as van der Waals spheres. The globular N-domain blocks the β-barrel of FepA (25).

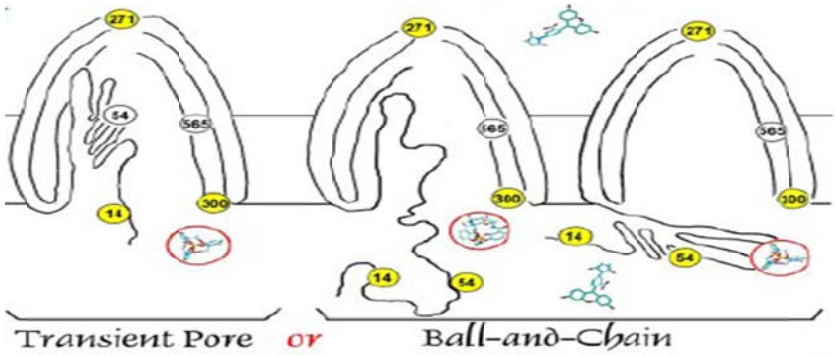

Figure 3. Two possible models of FeEnt transport through FepA. A graphical representation of the transient pore model where the N-domain of FepA is structurally rearranged within the FepA channel. In the ball-and-chain model the globular N-domain of FepA is displaced into the periplasmic space either as one large domain or unfolded. Figure provided by Ma, et al. (38).

In the ball-and-chain model, the N-domain of FepA is expelled into the periplasmic space in a concerted motion. The N-domain could be dislodged into the periplasm as a globule that is attached to the β-barrel by a “hinge-like” connection or by unfolding its α-β structure. This would form a ~ 40 Å OM channel for FeEnt to pass through. The drawback to this model would be the disruption of interactions within the N-domain and non-covalent interactions between the N-domain and the β-barrel wall (25).

In the transient pore model, the N-domain undergoes conformational change within the β-barrel of FepA during FeEnt transport. This would have to produce a passage way for FeEnt which must be at least 10 Å in diameter. In the transient pore model, it is unclear how a structural rearrangement could occur within the C-domain of FepA, considering the dense shape of the N-domain.

Chapter 2: Materials and Methods

The materials and methods listed here are frequently used assays. Procedures that are specific to one study are provided in the appropriate chapter.

Bacterial strains, plasmids, and culture conditions

The bacterial strains are derived from *E. coli* K-12 and are derivatives of BN1071 (10), which contains a wild type FeEnt uptake system. Tables 1 and 2 give a detailed list of the strains and plasmids, respectively. OKN3 (38) and OKN13 (38) were used as host strains for the low-copy plasmids pITS23 (39) or pITS47 (40), which contain a wild type gene for FepA that differ only in the restriction sites flanking *fepA*.

Table 1. Host strain

Strain	Relevent genotype or gene	Reference
BN1071	*F- thi entA pro trp rpsL*	Klebba 1982 (10)
OKN1	BN1071 *ΔtonB*	Ma 2007 (38)
OKN3	BN1071 *ΔfepA*	Ma 2007 (38)
OKN13	BN1071 *ΔtonB ΔfepA*	Ma 2007 (38)
OKN4	BN1071 *ΔfepB*	Newton 2010 (41)
OKN6	BN1071 *ΔfepC*	Newton 2010 (41)
OKN11	BN1071 *ΔfepD*	Newton 2010 (41)
OKN12	BN1071 *ΔfepG*	Newton 2010 (41)
OKN34	BN1071 *ΔfepA ΔfepB*	Newton 2010 (41)
OKN422	BN1071 *ΔfepB ΔtolC*	Newton 2010 (41)
CL29	*F- tfr-8* NbsB *thi-1rfaD*	Coleman 1979 (42)

Table 2. Plasmids

Plasmid	Relevent genotype or gene	Reference
pHSG575		Hashimoto-Gotoh 1981(43)
pITS23	*fepA*$^+$ on pHSG575	Scott 2001 (39)
pITS47	*fepA*$^+$ on pHSG575	Smallwood 2009 (40)

Bacteria were grown at 37°C in Luria-Bertani (LB) media. When necessary, strains were subcultured from stationary phase into iron-free MOPS minimal media (44). The antibiotics streptomycin (100 μg/mL) and chloramphenicol (10 μg/mL or 20 μg/mL) were added when required. When applicable, subcultures were conducted in the presence of a reducing agent, β-mercaptoethanol (1 mM).

Preparation of calcium chloride competent cells and heat shock transformation

A 5 mL overnight culture was grown in LB media with the appropriate antibiotics. Then the strain was subcultured 1:50 into 50 mL of LB in the presence of antibiotics and allowed to grow until mid-log phase, with an approximate A_{600nm} of 0.5-0.6. The cells were centrifuged at 4°C and 6,000xg for 10 minutes. After centrifugation the supernatant was discarded and the cell pellet was resuspended in 25 mL of ice cold 50 mM $CaCl_2$. This resuspension incubated on ice for 30 minutes before an additional centrifugation at 4°C and 6,000xg for 10 minutes. After centrifugation the supernatant was discarded and the cell pellet was resuspended in 0.5 mL ice cold 50 mM $CaCl_2$, 15% glycerol solution. The

resuspension was then separated into 40 µL aliquots, which were flash frozen in liquid nitrogen and immediately stored in a -80°C freezer. To prepare for transformation via heat shock, the competent cells thaw on ice, 4-6 µL of the plasmid were gently added and the cell mixture incubated on ice for 30 minutes. The cells were then heat shocked at 42°C for 40 seconds and placed back on ice for 2 minutes. Then 100-200 µL of super optimal broth with catabolite repression (SOC) media was added and the cells incubated at 37°C with shaking for 1 hour. The cells were then plated on LB plates with the appropriate antibiotics present. Colonies were picked 12-16 hours later.

Site-directed single cysteine substitution mutagenesis

QuikChange mutagenesis (Stratagene, San Diego, CA) was used to generate single cysteine mutations in *fepA* on pITS23 or pITS47. KAPA mutagenesis (Kapa Biosystems Inc., Woburn, MA) was also used to create single cysteine mutations in *fepA* on pITS47. DNA sequence analysis (MCLAB, San Francisco, CA or OMRF, Oklahoma City, OK) confirmed the cysteine substitution.

Siderophore nutrition assay

This was a modified qualitative assay of the ability of strains to grow in the presence of FeEnt when a chelator is present in the media (45). Strains were grown in LB media until late log phase in the presence of the appropriate antibiotics. A sample of 100 µL of bacterial culture, 3 mL of warmed Nutrient top agar containing 233 µM bipyridyl, and the

appropriate antibiotics was plated in 6-well plates. Once solidified, a sterile paper disc (6 mm in diameter) was placed in the center and 0.5 nmol of purified FeEnt (46) was added to the disc. The plates were incubated at 37°C overnight and the results were expressed as the diameter of growth around the discs. Additional experiments were conducted in the presence of a reducing agent, β-mercaptoethanol (βME), or an oxidizing agent, oxidized dithiothreitol (DTT), at various concentrations.

Colicin B sensitivity assay

To determine the sensitivity of a strain to Colicin B, a 100 µL overnight culture was added to 3 mL of warmed LB top agar and plated onto LB plates containing the appropriate antibiotic. Serial dilutions of purified Colicin B were done using half of a 96 well plate. Starting at the upper left well a 1:10 dilution was made down the column and 1:2 dilutions were made across the row. The serial dilution of Colicin B was applied on to the plate using a clonemaster. The plates were incubated at 37°C overnight and the titre was determined as the last Colicin B dilution able to clear the lawn of bacteria (26). Additional experiments were conducted in the presence of a reducing agent, β-mercaptoethanol.

Siderophore binding

This assay determined the about of ^{59}FeEnt that binds to FepA and was a modified version from previous experiments (23,27). Strains were subcultured at 1% from stationary phase LB cultures into MOPS minimal media and allowed to grow at 37°C for 5.5 hours or until late log phase.

When necessary, 1 mM βME was added to the subcultures. The binding experiments were conducted in triplicate at 0°C, which allowed ^{59}FeEnt to bind to FepA but did not allow uptake of the siderophore. The cell cultures, radioactive ligand, and appropriate buffers were all on ice while the experiment was conducted. ^{59}FeEnt was added to 10 mL MOPS, 0.4% glucose at the following concentrations: 0.05, 0.1, 0.5, 1.0, 5.0, and 10.0 nM ^{59}FeEnt (unless stated otherwise). These solutions were added to 100 µL aliquots of cell cultures and allowed to incubate for 5 seconds. The cells were then collected on 0.45 micron nitrocellulose filters and 10 mL of 0.9% LiCl was added to rinse the filter and prevent any further binding reactions. A gamma counter was used to analyze the extent of ^{59}FeEnt binding by detecting the counts per minute (cpm) of the cells. The specific activity of the ^{59}FeEnt and the OD_{600} of the cells were included when plotting the pmol of ^{59}FeEnt bound/10^9 cells versus the concentration of ^{59}FeEnt in a data fitting program. From these plots, the Kd and capacity could be determined. The negative control was done using a *fepA* deficient strain, OKN3. The positive controls were wild type strains BN1071 or OKN3 containing the plasmids pITS23 or pITS47. When relevant, fluorescent labeling of FepA occurred before binding assays to determine the effects of covalent modification by fluorophores.

Siderophore transport

To assay the uptake of ^{59}FeEnt, siderophore transport was conducted similarly to siderophore binding but the experiment was done at

37°C rather than 0°C. This allowed binding and uptake of ^{59}FeEnt to occur. This assay was also conducted in triplicate. To determine the uptake of ^{59}FeEnt, two separate incubation times were used, 5 seconds and 1 minute and 5 seconds. In some transport assays, the time points may vary. Although the 5 second measurement was done at 37°C, FeEnt transport did not occur because the passage through FepA occurs in 10-15 seconds (23,39,47,48). 100 µL aliquots of cells were mixed with 10 mL MOPS, 0.4% glucose containing various concentrations of ^{59}FeEnt, allowed to incubate at 37°C, collected on filters and rinsed with 0.9% LiCl. The uptake of ^{59}FeEnt in one minute was determined by calculating the difference of the counts at the two separate times. A plot of pmol ^{59}FeEnt/10^9 cells/minute versus the concentration of ^{59}FeEnt was used to determine the K_M and V_{max}. The negative and positive controls were OKN3, and BN1071 or OKN3 containing pITS23 or pITS47, respectively. When required, fluorescent labeling of FepA occurred before ^{59}FeEnt transport assays to determine the effects of fluoresceination.

Siderophore accumulation

To measure the accumulation of ^{59}FeEnt in bacteria, strains were subcultured at 1% from stationary phase LB cultures into MOPS minimal media and allowed to grow at 37°C until late log phase. When required, subcultures were conducted in the presence of 1 mM β-mercaptoethanol. For accumulation of the siderophore to occur, the assay was done at 37°C to allow ^{59}FeEnt binding and uptake. An aliquot of the cells were taken and

placed in a 37°C shaking water bath and ^{59}FeEnt was added to the cells to a final concentration of 5 μM ^{59}FeEnt. The high concentration of ^{59}FeEnt was essential to ensure that depletion of the siderophore would be minimal over an extended period of time. Aliquots of the cells (100 μL) were collected on nitrocellulose filters and rinsed with 0.9% LiCl after specific incubation periods: 5, 15, 25, 45, and 60 minutes. This was done in triplicate and the filters were counted to determine the accumulation of ^{59}FeEnt in the bacteria over various periods of time.

Fluorescence labeling of FepA Cys sites *in vivo*

The substituted Cys sulphydryl groups in FepA were conjugated to the Cys specific fluorophores, fluorescein maleimide (FM) (49). Cells were subcultured in MOPS minimal media and allowed to grow for 5.5 hours or until late log phase. The OD_{600} was measured and 5 x 10^8 cells were collected by centrifugation at 17,000xg for 1 minute at 4°C. The cells were then washed and resuspended in 1 mL of 50 mM Na_2HPO_4, pH 6.5, 0.9% NaCl, containing 0.4% glucose. The cells were incubated for 10 minutes at 37°C. FM was then introduced to the cells at 5-10 μM and the cells were incubated for an additional 15 minutes at 37°C. At the end of the labeling period, the reactions were quenched with 1 mM cysteine or 2 mM βME. The cells were washed three times with 1 mL 50 mM of Na_2HPO_4, pH 6.5, 0.9% NaCl. For spectrophotometric studies, the cells were finally resuspended in 1 mL TBS (50 mM Tris chloride, pH 7.4, 0.9% NaCl), 0.4% glucose. For detection of fluorescence labeling by SDS-PAGE, 1 x 10^8

bacteria were lysed by boiling for 5 minutes in SDS-PAGE sample buffer before resolution by SDS-PAGE. A modified procedure of fluorescence labeling was used for FRET experiments that can be found in chapter 4.

Detection of fluorescence labeling by SDS-PAGE and expression of FepA

After SDS-PAGE was completed the gel was scanned for fluorescence on a STORMSCAN phosphorimager (Molecular Dynamics). The proteins in the gel were transferred to nitrocellulose paper using a semi-dry transfer apparatus. The blots were developed with mouse anti-FepA monoclonal antibodies (mAb) 41 and 45 (46) and ^{125}I-protein A (23). The blots were then exposed on an imaging screen and the radioactivity was quantified on the STORMSCAN phosphoimager. All of the scanned images were then analyzed by ImageQuant 5.2 (Molecular Dynamics).

Protein expression

To determine and compare the expression of wild type and mutated FepA, western immunoblots were conducted. After SDS-PAGE was complete the proteins in the gel were transferred to nitrocellulose paper using a semi-dry transfer apparatus. The blot was blocked with TBS plus 1% gelatin for 15 minutes and then incubated with mouse anti-FepA mAb 41 and mAb 45 in TBS plus 1% gelatin for a minimum of one hour. Either water or TBS and 0.05% tween 20 was used to wash the blot with three five minute washes. After the wash, the blot was incubated with ^{125}I-

protein A for a minimum of two hours. The blot was then exposed on an imaging screen and the blot was visualized using a StormScanner.

Chapter 3: Direct measurements of FepA during FeEnt transport through post-uptake binding experiments

Background

The role of TonB is still unknown but it is essential for most ligand-gated porin transport, exceptions being T5 through FhuA (50) and cloacin DF13 through IutA (51). The necessity of TonB for the transport of all metal complexes through the OM creates questions concerning the proportion of TonB and TonB-dependent transporters present in the cell. In iron-deficient conditions, the total concentration of *E. coli* TonB-dependent receptor proteins are present in the OM ~100-fold greater than that of TonB in the IM (52,53). This suggests that all of the OM TonB-dependent transporters could not be active at the same time because TonB could not associate with all of the TonB-dependent proteins in the OM.

The overall rate of FeEnt uptake is relatively low (kcat ~ 5 min^{-1}) (39,47,48). Could this be due to the fact that there is only a portion of FepA proteins that can associate with TonB or could this result from an intrinsically slow transport mechanism? By observing the transport of FeEnt through FepA using the assay, post-uptake binding, we can address this and other questions. We used this assay to observe wild-type cells and strains lacking TonB, FepB, FepD, FepG, and TolC. FeEnt transport measurements were taken alone and during simultaneous transport of ferrichrome (Fc).

Experimental Procedures

Siderophore post-uptake binding (PUB)

Siderophore post-uptake binding determined the quantity and fraction of active FepA proteins by modifying the previous methods of siderophore binding and transport. This was done by taking advantage of the binding and transport temperatures, 0°C and 37°C, respectively. At 0°C, bacterial cells were saturated with ^{56}FeEnt and this ensured only the binding of ^{56}FeEnt to FepA would occur. Once the temperature was increased to 37°C, all of the bound ^{56}FeEnt would be transported through FepA. This allowed FepA to be ligand free and the addition and measurement of ^{59}FeEnt determined the fraction of active FepA. Figure 4 illustrates the various types of binding essential in this study. This assay was independent of the uptake of the ferric siderophore through the IM into the cytoplasm; therefore it focused on the transport of FeEnt through the OM alone.

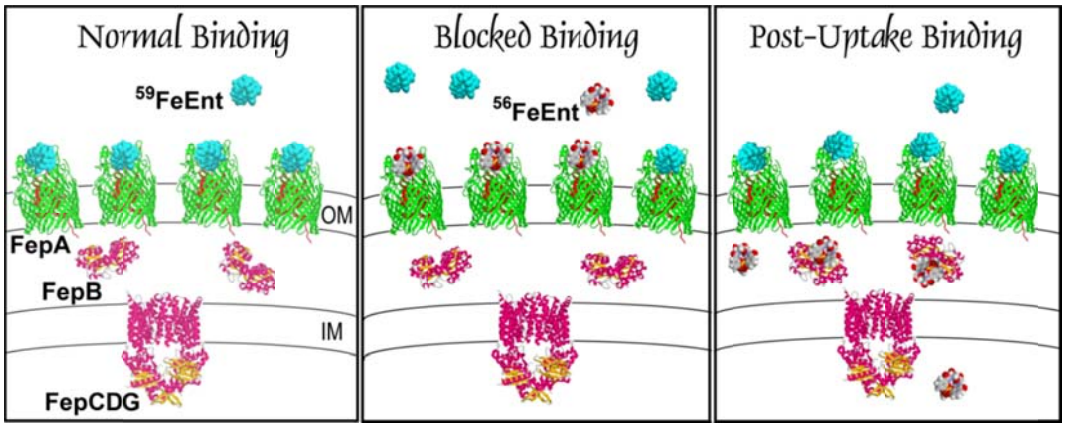

Figure 4. Representation of normal, blocked, and post-uptake binding assays of FepA mediated FeEnt transport. In this graphic, the molecules are not drawn to scale. Shown in the figures are FepA (PDB entry 1FEP), FepB (model based on the structure of *Haemophilus influenzae* Fpb, PDB entry 1D9V), FepCDG (based on the structure of the *H. influenzae* ABC-transporter, PDB entry 2N2Q), ^{59}FeEnt (cyan), and ^{56}FeEnt (CPK colors). Normal binding assays (**left panel**) were done at 0°C and ^{59}FeEnt was introduced to bacterial cells. This determined the ^{59}FeEnt binding capacity. In blocked binding assays (**center panel**) bacterial cultures were first exposed to excess ^{56}FeEnt, saturating FepA proteins. Cells were then pelleted by centrifugation and resuspended at 0°C this allowed re-equilibration of the binding interactions, dissociation of FepA and FeEnt could occur during this period. ^{59}FeEnt was then added to the cells and the amount of ^{59}FeEnt bound revealed the number of ligand-free FepA proteins. This was relative to the normal binding results and thereby revealed the number of remaining ligand bound FepA as well. Post-uptake binding (**right panel**), is similar to blocked binding but after saturation of ^{56}FeEnt, the temperature was increased to 37°C allowing FepA transport of ^{56}FeEnt. ^{59}FeEnt was then introduced to the cells at 0°C, to determine the amount of FepA proteins active during the transport incubation period. These measurements were also relative to the blocked binding results.

The cells were subcultured in MOPS minimal media as described in siderophore binding. The MOPS cultures were collected in 1 mL aliquots into microcentrifuge tubes and allowed to incubate on ice for 20 minutes. After this incubation period, ^{56}FeEnt was added to the bacteria to a final concentration of 100 nM. To remove excess ^{56}FeEnt, the cells were

pelleted by centrifugation at 4°C for 3 minutes and the supernatant was removed. The pellet was then resuspended in 100 µL of ice-cold MOPS media. Uptake of ^{56}FeEnt occurred by the addition of 900 µL of MOPS media at 42°C and incubating the bacteria for 1 minute at 37°C. The cells were then chilled on ice and pelleted. The pellet was resuspended in 1 mL of ice-cold MOPS media. 100 µL aliquots of cells were mixed with 10 mL of ice-cold MOPS media containing varying concentrations of ^{59}FeEnt. The bacteria were collected and rinsed on nitrocellulose filters. The filters were then measured using a gamma counter.

PUB assays were also done in the presence of ferrichrome (Fc). Bacterial cells were grown, chilled, and then mixed with saturating amounts (100 nM) of both ferric siderophores. The excess siderophores were removed by centrifugation and the pellet was resuspended in 100 µL of MOPS media containing 100 nM Fc. The cells began ferric siderophore transport once 900 µL of MOPS media at 42°C was added and the cells were allowed to incubate at 37°C for 1 minute. Subsequent binding of ^{59}FeEnt determined the amount of ^{56}FeEnt uptake during the 1 minute incubation period.

To appropriately determine the fraction of active FepA proteins additional control experiments were required. One control was the aforementioned siderophore binding assay using ^{59}FeEnt to determine the total ^{59}FeEnt binding capacity. The other control was a blocked binding assay that measured ^{59}FeEnt binding at 0°C to cells previously saturated

with ^{56}FeEnt at 0°C. This assay measured the amount of ^{56}FeEnt that dissociated from the bacteria.

Immunoprecipitation

To determine if FepB interacted with FepA at the periplasmic surface of the outer membrane, purified FepA (54) was immunoprecipitated with an IgG2b monoclonal antibody in the presence of purified FepB (55) and FeEnt. The mouse anti-FepA monoclonal antibody mAb 45 recognized loop 4 of FepA (26) and inhibited FeEnt adsorption and uptake (46), but previous flow cytometric analyses showed that the binding of FeEnt to FepA did not block the interaction of mAb 45. To remove precipitates, the solutions of FepA, mAb 45, and FepB were centrifuged at 18,000xg for 5 minutes before immunoprecipitation. FepA (4.5 µg) was incubated with or without FeEnt (10 nM) for a few seconds and FepB (15.4 µg) and mAb 45 (30 µg) were added in a final volume of 0.5 mL of TBS. The suspension sat overnight at 4°C and then 50 µL of protein A-agarose (3 mg/mL resin) was added and the mixture incubated for an additional 2 hours at room temperature. The immune complexes were pelleted by centrifugation at 2,500xg for 3 minutes and solubilized in SDS sample buffer and analyzed by SDS-PAGE. To analyze the SDS-PAGE results properly, additional conditions were tested during immunoprecipitation.

Radioisotopic FeEnt retention assays

Retention assays determined the retention of ^{59}FeEnt during subsequent exposure to ^{56}FeEnt. The bacterial strains were exposed to 0.5 μM ^{59}FeEnt for 40 minutes and then ^{56}FeEnt was added to 10 μM. Similar to accumulation measurements, aliquots of the cells were taken at various times, filtered, washed, and counted to determine the retention of ^{59}FeEnt.

Determination of the activation energy of FeEnt transport through FepA by *in vivo* fluorescence analysis

To determine the activation energy of FeEnt transport through FepA we fluorescently labeled OKN3/pFepAS271C (38,49) with FM using the protocol mentioned in methods and materials. We spectroscopically measured 5 x 10^6 cells with FeEnt in an SLM-AMINCO 8000 fluorometer upgraded to 8100 functionality. We were able to observe the quenching of FM by FeEnt when we measured the emission wavelength at 518 nm with an excitation wavelength of 490 nm. When FeEnt was bound to FepAS271C-FM, the fluorescence emissions quenched and as the bacteria depleted the FeEnt present in the solution by transport, the fluorescence recovered (49). From these measurements, we were able to determine the rate constants for the transport of FeEnt through FepA in two ways.

In the first method (time to depletion threshold), the cells were saturated with 10 nM FeEnt and we measured the time for the cells to deplete the FeEnt from solution.

$$\mathrm{FepA} + \mathrm{FeEnt_{out}} \underset{k_{-1}}{\overset{k_1}{\rightleftharpoons}} \mathrm{FepA{-}FeEnt} \xrightarrow{k_2} \mathrm{FepA} + \mathrm{FeEnt_{in}}$$

$$v = k_2[\text{FepA-FeEnt}] \qquad \text{(Eq. 1)}$$

FeEnt was in excess, therefore $v = V_{max}$ and [FepA-FeEnt] = [FepA]. So equation 1 can be modified as:

$$V_{max} = k_2[\text{FepA}] \qquad \text{(Eq. 2)}$$

We calculated the V_{max} by measuring the time (s) from the addition of FeEnt until F/F_0 recovered to an arbitrary value of 0.4. At this point ~20 pmol of FeEnt were transported by the cells. By determining the V_{max} at various temperatures and at a concentration of 5 nM FepA, we were able to calculate k_2.

In the second method, we observed the rate of depletion. The bacteria continued transport thereby decreasing the concentration of FeEnt in solution. As a result, FepAS271C-FM had a linear fluorescence recovery and the fluorescence emissions returned to its original level. The midpoint of the unquenching curve was considered the point at which the FepA is half-saturated with FeEnt, making the following equation true.

$$v = \frac{V_{max}}{2} = \frac{k_2[\text{FepA}]}{2} \qquad \text{(Eq. 3)}$$

Using this method, the slope of the unquenching curve was proportional to v, and because the concentration of FepA was 5 nM, we were able to

determine k_2. By plotting ln(k_2) versus 1/T, we were able to determine the activation energy (E_a) from the Arrhenius equation, $k = Ae^{-\frac{E_a}{RT}}$. Although these calculations were approximations, the values of k_2 derived from the two separate methods proportionally reflected the temperature dependence of FeEnt transport.

Results

Fraction of FepA proteins that transport FeEnt

PUB experiments were conducted to calculate the fraction of FepA proteins that could participate in FeEnt uptake at any time. FepA proteins were saturated with ^{56}FeEnt and allowed to transport. Of the portion that were able to transport, the FepA proteins became vacant and were able to bind ^{59}FeEnt.

Because it was possible that the FeEnt bound to FepA could dissociate, we measured the dissociation by blocked binding assays. The strains BN1071 (contains wild type FeEnt transport system (10)) and OKN1 (*ΔtonB*) (38) were studied. These cells were incubated on ice with excess ^{56}FeEnt and collected by centrifugation and resuspended in ice-cold buffer. The cells were then mixed with ^{59}FeEnt to determine the amount of FepA that had dissociated with ^{56}FeEnt. The results of the blocked binding assay revealed that about two-thirds of the FepA proteins were still bound to ^{56}FeEnt (Fig. 5).

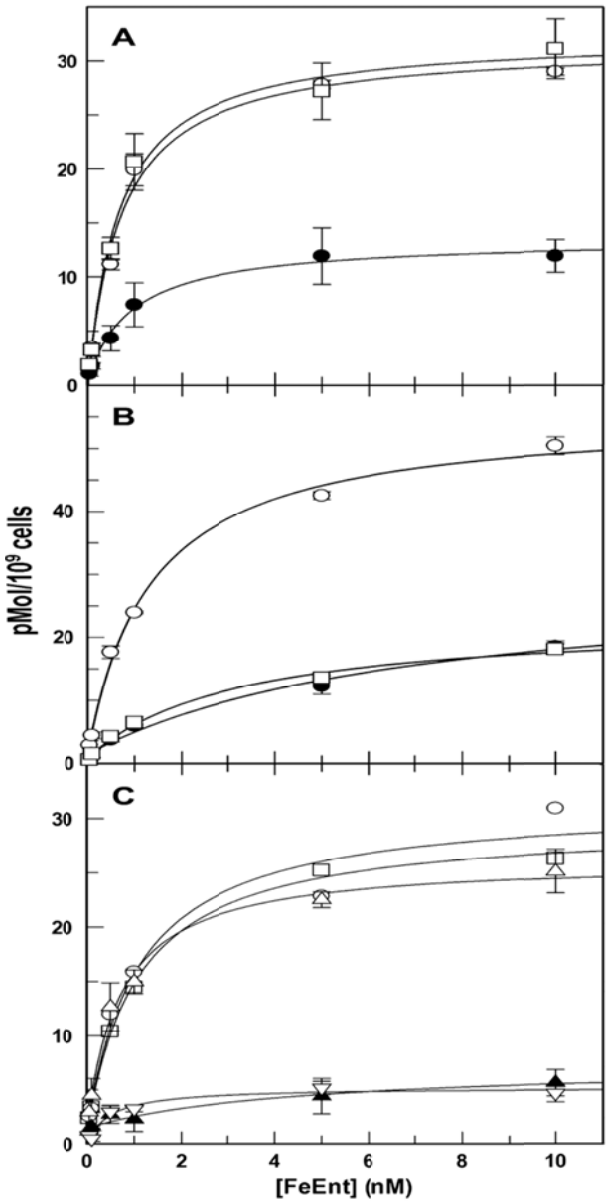

Figure 5. PUB measurements of FeEnt uptake with and without *tonB* in the absence and presence of CCCP. In **panel A** BN1071: *tonB*$^{+}$ was assayed under three conditions: normal binding (○), blocked binding (●), and PUB (□). In **panel B** OKN1: Δ*tonB* was assayed under the same conditions. In **panel C**, BN1071 was assayed for normal binding (○) and PUB (□), but also assayed after a 30 minute exposure to 0.5 mM CCCP, normal binding (△), blocked binding (▲), and PUB (▽). In panel C, error bars were only shown for the CCCP-treated samples. Unless stated otherwise, error bars represent the standard error.

Both strains tested showed that a third of the FepA proteins dissociated ^{56}FeEnt. In the wild type strain, the PUB assay showed that the remaining two-thirds of FepA that were bound to ^{56}FeEnt were able to transport the siderophore and ^{59}FeEnt was able to bind to FepA to full capacity. OKN1 lacks *tonB*; therefore we considered it a negative control for FeEnt uptake. Figure 5 showed the results of OKN1 in all three binding conditions. As expected the blocked binding and PUB results were almost identical. The results indicated that in the PUB experiment, the remaining two-thirds of FepA associated with ^{56}FeEnt were unable to transport during the 37°C temperature increase and only the dissociated FepA proteins were able to bind ^{59}FeEnt. BN1071 treated with the proton motive force inhibitor, carbonyl cyanide m-chlorophenyl hydrazone (CCCP), showed similar results to OKN1 and could not uptake ^{56}FeEnt.

Initial rate of FeEnt uptake by FepA

The use of PUB assays allowed for the direct measurement of OM transport, which differed from standard radioisotopic iron uptake assays. The latter allowed the accumulation of ^{59}FeEnt within the cell, thereby measuring the amount of ^{59}FeEnt present in the cytoplasm, periplasmic space, and the OM. The results of the PUB assays indicated that uptake occurred immediately once transport was allowed and continued until all FepA proteins were vacated (Fig. 6). The transport reaction was a first order reaction with k = 1.2 min^{-1}. This rate is 3-fold slower than previously measured. The discrepancy may be due to the differences in the methods

employed. Previous assays were done at 37°C and the cells never experienced a temperature change. In PUB assays, the cells were chilled on ice with the iron siderophore present and to induce transport the cells were rewarmed to 37°C. To test this theory, conventional ^{59}FeEnt uptake assays were conducted with cells that were chilled prior to transport and for the first 20 seconds the calculated V_{max} was 83 pmol(10^9 cells·min)$^{-1}$ for the next 40 seconds the rate increased to 172 pmol(10^9 cells·min)$^{-1}$. Previous studies have shown that with conventional radioisotopic assays the V_{max} was 208 pmol(10^9 cells·min)$^{-1}$ (47). Chilling the cells prior to transport resulted in turnover numbers of 1.2 min^{-1} for the first 20 seconds, 2.6 min^{-1} for the next 40 seconds, and an average of 2 min^{-1} for the 1 minute assay period. These results explained the lower rate determined by the PUB assays.

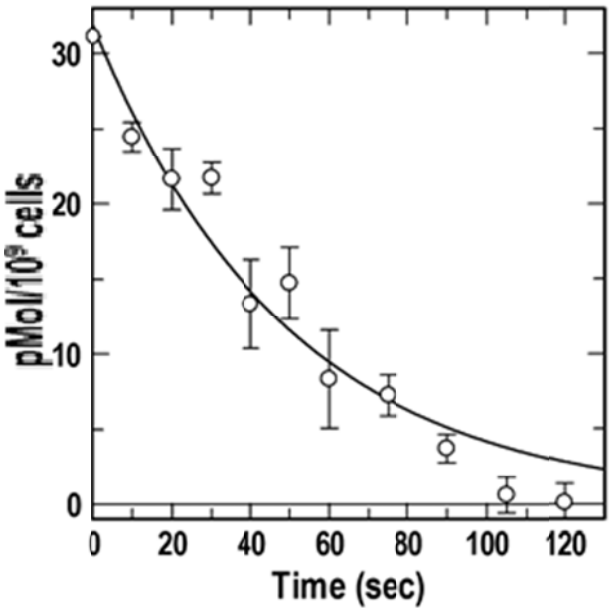

Figure 6. Initial kinetics of FeEnt OM from PUB assays. BN1071 was chilled on ice and saturated with ^{56}FeEnt in 100 µL of ice-cold MOPS. The cells were then warmed to 37°C by the addition of 1 mL MOPS media at 42°C. At 10 second intervals, aliquots were removed and the cells were diluted by 250-fold with ice-cold MOPS. After 5 minutes, ^{59}FeEnt was added to the cells to 25 nM. To determine the extent of ^{59}FeEnt binding, the cells were filtered, washed, and counted. The results (○) plotted were depicted as the depletion of bound ^{56}FeEnt to the OM protein FepA.

Kinetics of ^{59}FeEnt accumulation

We conducted ^{59}FeEnt accumulation assays with BN1071 over a 90 minute period. Enough ^{59}FeEnt (10 µM) was present in the experiment to ensure the siderophore was in excess during the assay. The data indicated that were three uptake stages (Fig. 7): an initial phase at a maximum rate during the first 30 seconds (V_{max} =150 pmol(10^9 cells·min)$^{-1}$), a secondary phase in the following 10 minutes with an intermediate rate (V_{max} = 78 pmol(10^9 cells·min)$^{-1}$), and finally a steady state phase with

the lowest rate (V_{max} = 37 pmol(10^9 cells·min)$^{-1}$) that continued until the end of the 90 minute period.

To investigate the triphasic time course seen in the accumulation assays, we conducted PUB assays at three separate times, 15 seconds, 5 minutes, and 25 minutes (Fig. 7). The results supported the presence of three different uptake rates. Immunoblots were done on these samples and the concentrations of FepA between the samples were similar. These results suggested that the decrease in transport rate through FepA caused the drop in the overall ferric enterobactin accumulation into the cytoplasm. If this was true, it was possible that the OM transport activity of FepA was regulated by other cell envelope or intracellular processes.

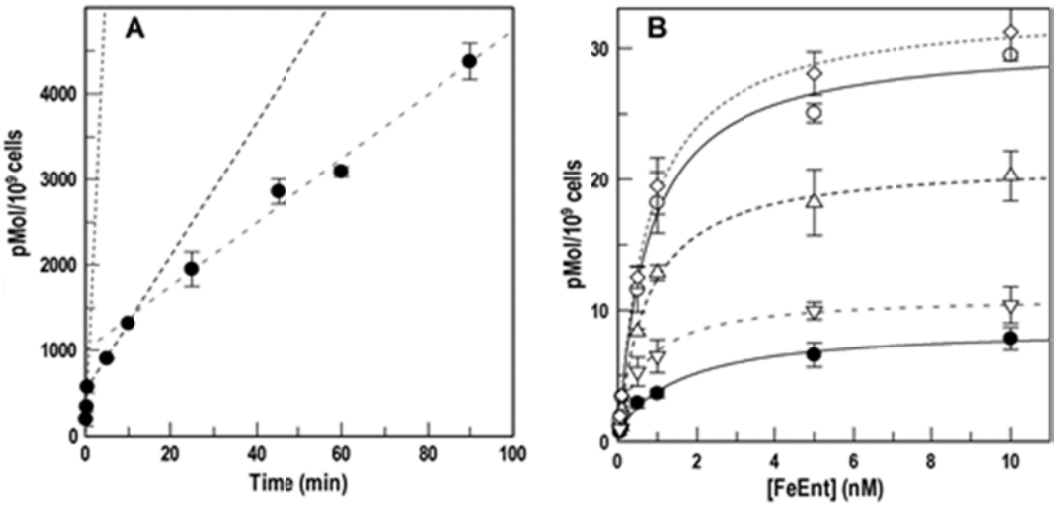

Figure 7. Three FeEnt uptake stages. ^{59}FeEnt accumulation assays were conducted with BN1071 (**panel A**) and aliquots were removed and counted over a 90 minute period (●). Fitted curves (····, - - - -, – – – –) indicated the presence of three uptake stages, initial, secondary, and final, respectively. PUB measurements of BN1071 (**panel B**) were done with a total of 10 μM ^{56}FeEnt present at t = 0. Aliquots of the cells were collected, centrifuged, resuspended, and incubated at 37°C for 1 minute before the addition of the siderophore, 5 and 20 minutes afterward. Then ^{59}FeEnt was added over a range of concentrations. Normal binding (○), blocked binding (●), and PUB at t = 0 (◇), 5 min (△), and 25 min (▽). The experiment supported three different rates of FeEnt uptake at t = 0 (••••), 5 min (- - - -), and 20 min (– – – –).

FepA-mediated FeEnt uptake in bacteria devoid of FepB, FepD, and FepG

In-frame deletions were engineered (56) to remove *fepB, fepD,* and, *fepG* loci in BN1071 and the deletions were verified by DNA sequence analysis. We conducted siderophore nutrition tests and ^{59}FeEnt accumulation assays and the strains were inactive and unable to accumulate the ^{59}FeEnt, respectively (data not shown). To analyze the effect of the deletions on FeEnt transport, we took PUB measurements on

all three strains. The results indicated that none of the strains were able to uptake ^{59}FeEnt through FepA (Fig. 8).

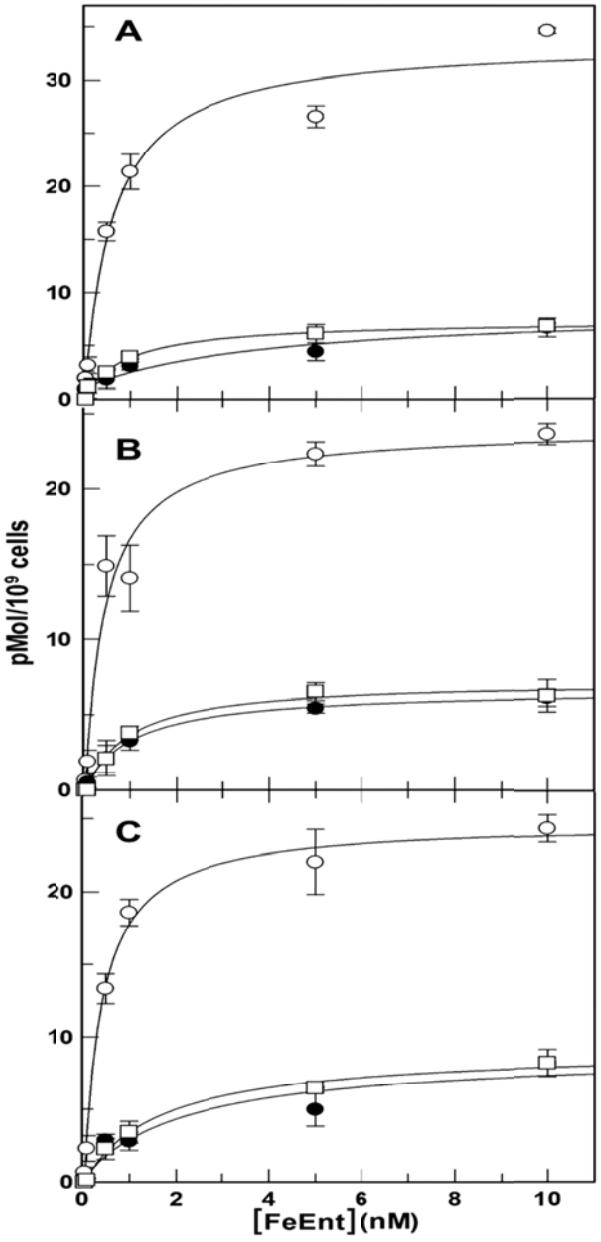

Figure 8. PUB assays of strains lacking FepB, FepD, or FepG. PUB measurements were done with OKN4 (*ΔfepB*, **panel A**), OKN11 (*ΔfepD*, **panel B**), and OKN12 (*ΔfepG*; **panel C**). Normal ^{59}FeEnt binding (○), blocked binding (●), and PUB (□) conditions were tested on the three strains.

The impaired FeEnt uptake through the OM was unexpected and it raised questions about the interactions between FepB and FepA. The role of FepB is to shuttle FeEnt from FepA to the inner membrane permease complex FepCDG. But, it was unknown whether an interaction between FepB and FepA occurred during FeEnt transport. To determine if an interaction between the two proteins occurred, we conducted immunoprecipitation experiments. By using an antibody that recognizes an epitope in loop 4 of FepA (anti-FepA mAb 45), we tested whether or not FepB would precipitate along with FepA in the presence or absence of the iron siderophore. As seen in Fig. 9, FepB did not co-precipitate with FepA, mAb45, and protein A-agarose in the absence or presence of FeEnt (10 nM). We conducted an additional experiment with FepB and FeEnt that included FepA in OM fragments (54). The samples were precipitated by ultracentrifugation and the same results were seen (Fig. 10). Both assays indicated that FepB did not actively interact with FepA during FeEnt transport through the OM.

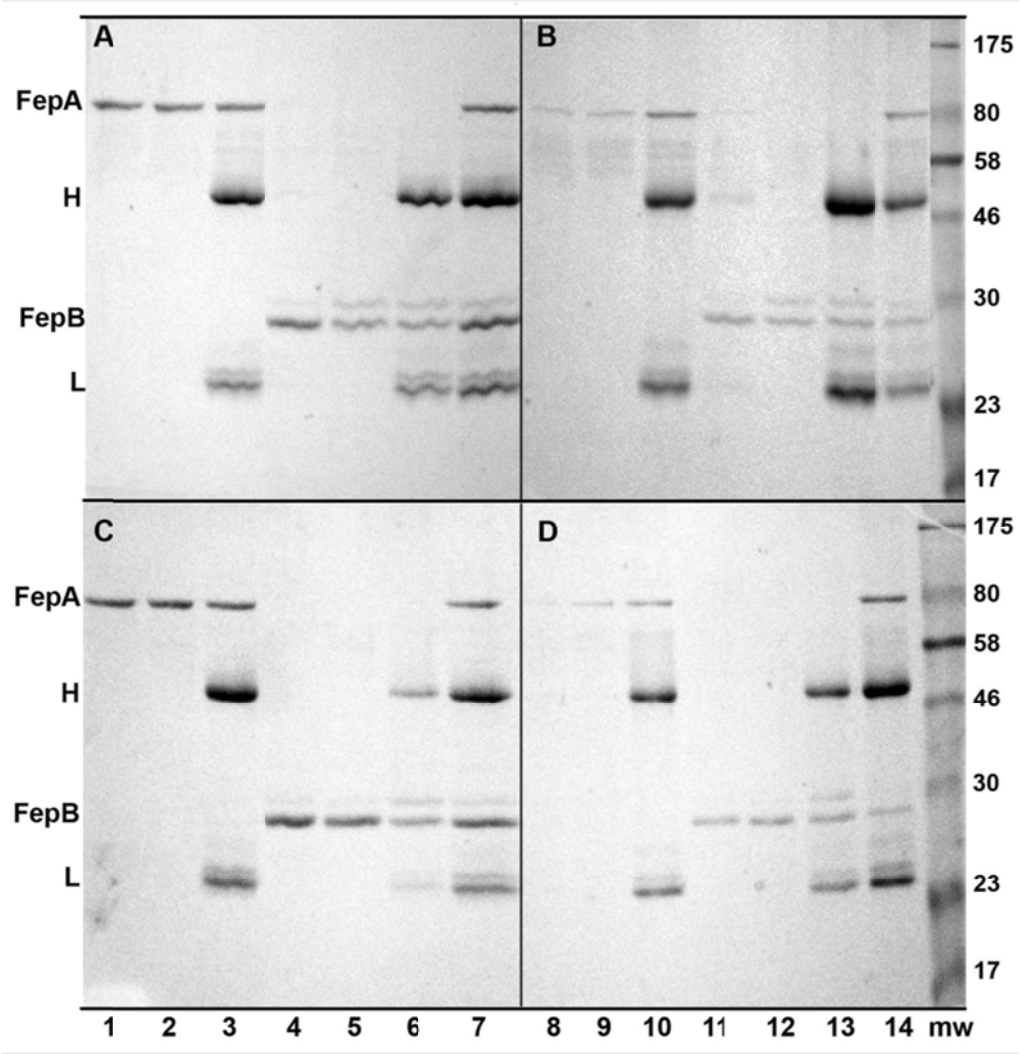

Figure 9. Immunoprecipitation of FepA in the presence of FeEnt and FepB. Purified FepA was incubated in the absence (**panels A and B**) and presence of 10 nM FeEnt (**panels C and D**). The solutions were mixed with anti-FepA mAb 45 with or without FepB present. Protein A-agarose (PAA) was added to the mixture after the reaction incubated overnight. These reactions were allowed to incubate for an additional 5 hours and the precipitates were collected by centrifugation at 2,500xg for 3 minutes. The supernatants (lanes 1-7) and resuspended pellets (lane 8-14) were analyzed by SDS-PAGE and visualized by coomassie stain (57). Lanes 1, 8: FepA; lanes 2, 9: FepA + PAA; lanes 3, 10: FepA + PAA + mAb45; lanes 4, 11: FepB; lanes 5, 12: FepB + PAA; lanes 6,13: FepB + PAA+ mAb45; lanes 7, 14: FepB + PAA + mAb 45 + FepA. The heavy (H) and light (L) chains of the antibody were seen in the gels as well.

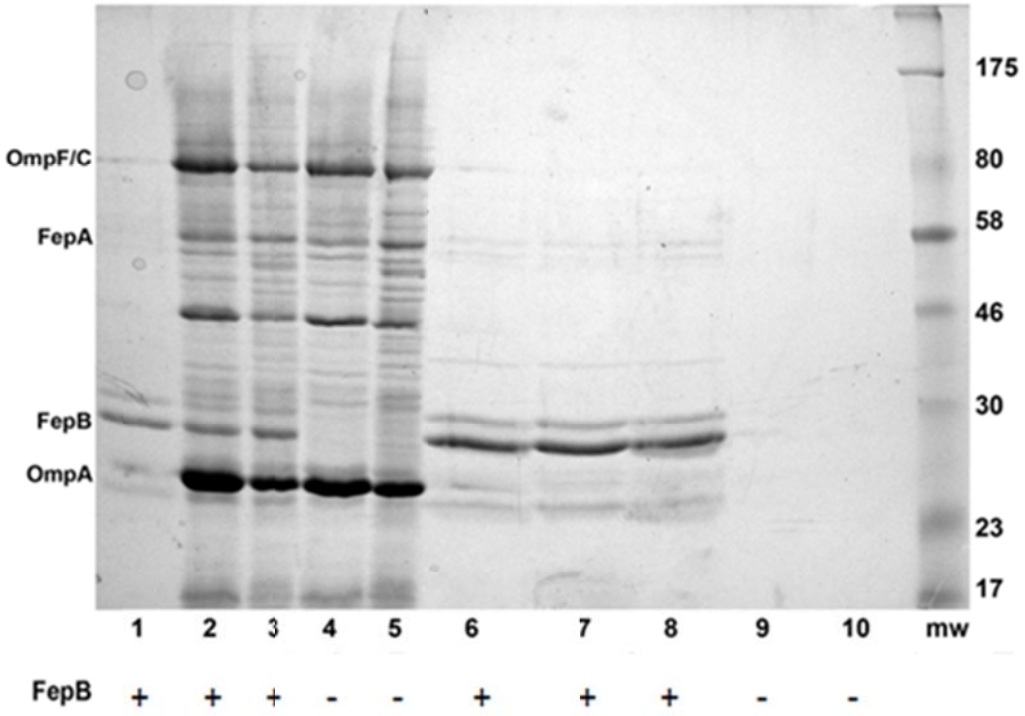

Figure 10. Precipitation of OM fragments containing FepA in the presence of FeEnt and FepB. BN1071 was grown in MOPS minimal media and saturated with FeEnt before lysing the cells. The OM fractions were purified by sucrose gradient fractionation (58). The pellet that formed through the sucrose gradient (lanes 2, 4, 7, 9) and the OM band suspended in the gradient (lanes 3, 5, 8, 10) were tested with purified FepB (lanes 1 and 6) to determine if FepB would interact with FepA. The OM pellets and OM fragments were mixed with FepB and incubated on ice for 30 minutes. The samples were then centrifuged at 100,000xg for 45 minutes. The pellets (lanes 1-5) and the supernatant (6-10) were analyzed by non-denaturing SDS-PAGE and visualized by coomassie stain (samples were not boiled for better visualization of FepB). FepB mostly remained in the supernatant during ultracentrifugation.

To investigate the active role of FepB during FeEnt transport through FepA, we conducted site-directed fluorescence spectroscopy. Previous studies showed that the Cys substituted mutant in FepA, G54C, was able to be modified by FM during FeEnt transport (38). G54C was not labeled in strains lacking *tonB* or in energy-poisoned cells. We introduced

pFepAG54C into OKN3 (*ΔfepA*), OKN34 (*ΔfepA*, *ΔfepB*), and OKN13 (*ΔtonB*, *ΔfepA*), strains and conducted and compared FM labeling of G54C (Fig. 11 panel A). FM was able to modify G54C when FeEnt was present whether or not the strain had *fepB*. In previous experiments, G54C was not conjugated to FM in the *ΔtonB* host. These results suggested that FeEnt transport through FepA could occur in the absence of FepB.

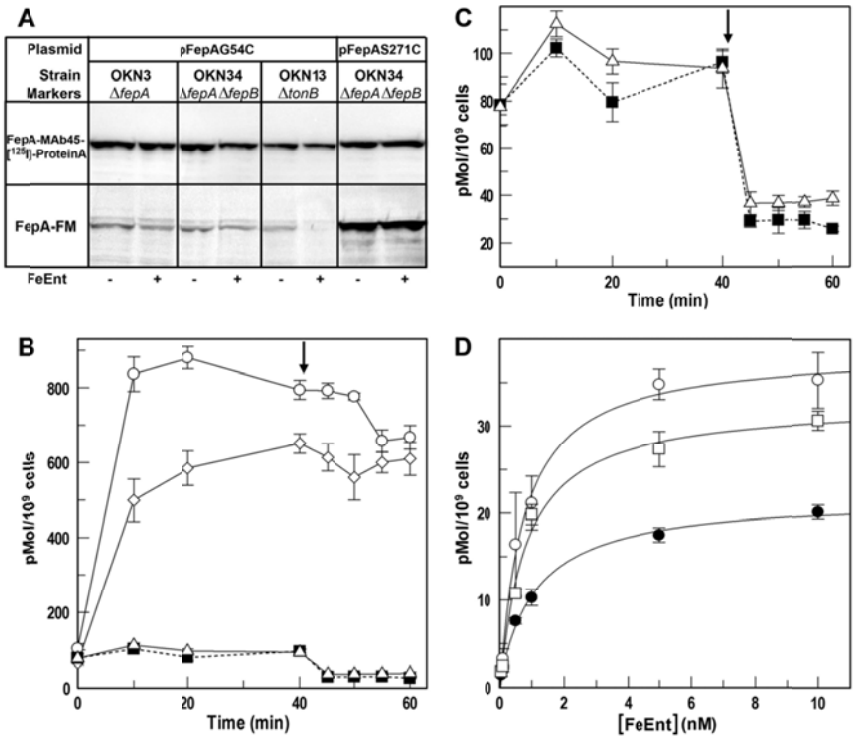

Figure 11. Fluorescence labeling during FeEnt uptake, accumulation and PUB measurements. To determine the effect of FeEnt uptake on fluorescent labeling of pFepAG54C or pFepAS271C, OKN3 (*ΔfepA*), OKN34 (*ΔfepA*, *ΔfepB*), and OKN13 (*ΔtonB*, *ΔfepA*) were used as host strains for pFepAG54C or pFepAS271C (**panel A**). The cells were labeled with 5 μM FM in the presence of 10 μM FeEnt at 37°C. After FM labeling, the samples were analyzed through SDS-PAGE to determine the extent of fluorescence (bottom lanes). To compare the FepA expression in all of strains and conditions, the proteins in the gel were then transferred and immunobloted with anti-FepA (top lanes). BN1071 (○), OKN1 (*ΔtonB*) (■), OKN4 (*ΔfepB*) (△), and OKN422 (*ΔfepB*, *ΔtolC*) (◇) were tested to determine the retention of ^{59}FeEnt after exposure to ^{56}FeEnt (**panel B**). Initially, the samples were exposed to 0.5 μM ^{59}FeEnt. After 40 minutes, ^{56}FeEnt was added to 10 μM. To determine the retention of ^{59}FeEnt, aliquots of the cells were taken at various times, filtered, washed, and counted. A drop in ^{59}FeEnt retention after the addition of ^{56}FeEnt was seen in the strains without *tonB* and *fepB* (**panel C**). Post-uptake binding assays were done with OKN422 (**panel D**) to determine if the deletions of *fepB* and *tolC* would affect FeEnt transport through FepA. Normal ^{59}FeEnt binding measurements (○), blocked binding assays (●), and PUB (□) determinations were done on OKN422 to properly assess the effects of the deletions.

The PUB assays with OKN4 suggested that FepB was essential in the uptake of FeEnt through the OM but the FM results with G54C indicated that FeEnt uptake was occurring through FepA, despite the *fepB* deletion. To provide additional insight in the differing results, we studied ^{59}FeEnt retention assays. BN1071 (wild type), OKN1 (*ΔtonB*), and OKN4 (*ΔfepB*) were subjected to retention assays (Fig. 11 panel B and C) similar to those done with BtuB (35). The bacterial strains were initially exposed to ^{59}FeEnt and then excess ^{56}FeEnt was added to determine the retention of the radioactive FeEnt. As expected, the wild type strain was able to retain ^{59}FeEnt after ^{56}FeEnt exposure. The *ΔfepB* strain did not bind or retain as much ^{59}FeEnt as BN1071. This suggested that without the periplasmic binding protein, FepB, FeEnt did not stay internalized and was released into the media.

Previous studies of TolC by Bleuel, et al., indicated that TolC was involved in the efflux of FeEnt across the OM of *E. coli* (59). The *ΔfepB* and *ΔtolC* strain, OKN422, was generated to determine if TolC was involved in the release of siderophore in the absence of the periplasmic binding protein. OKN422 was also subjected to ^{59}FeEnt retention determinations and the results were similar to the wild type strain BN1071. We also conducted PUB measurements on OKN422 (Fig. 11 panel D). The results indicated that FepA was able to transport FeEnt across the OM even in the absence of FepB to bind the siderophore in the perisplasmic space. The retention and PUB measurements confirmed the

involvement of TolC in the efflux of FeEnt. Strains lacking *fepB* accumulated FeEnt within the perisplasmic space during FeEnt transport and TolC was responsible for the release of FeEnt through the OM.

Simultaneous TonB-dependent uptake of two ferric siderophores

TonB is necessary for the transport of all iron siderophores through the OM. TonB interacts with the TonB box of OM receptor proteins. Because of this interaction and proportion of TonB and TonB-dependent receptor proteins, the simultaneous transport of various ferric siderophores should competitively inhibit the individual rates of siderophore internalization. To determine the effect of FeEnt uptake in the presence of saturating Fc, we conducted PUB measurements and conventional ^{59}FeEnt assays (Fig. 12). The standard ^{59}FeEnt uptake assays indicated that the presence of saturating Fc had little effect on FeEnt transport. PUB assays showed a 20% decrease in the V_{max} of FeEnt uptake when saturating Fc was present. The results of standard siderophore uptake assays for ^{59}Fc transport in the presence of saturating FeEnt indicated that the V_{max} of ^{59}Fc was reduced by 50% in the presence of FeEnt.

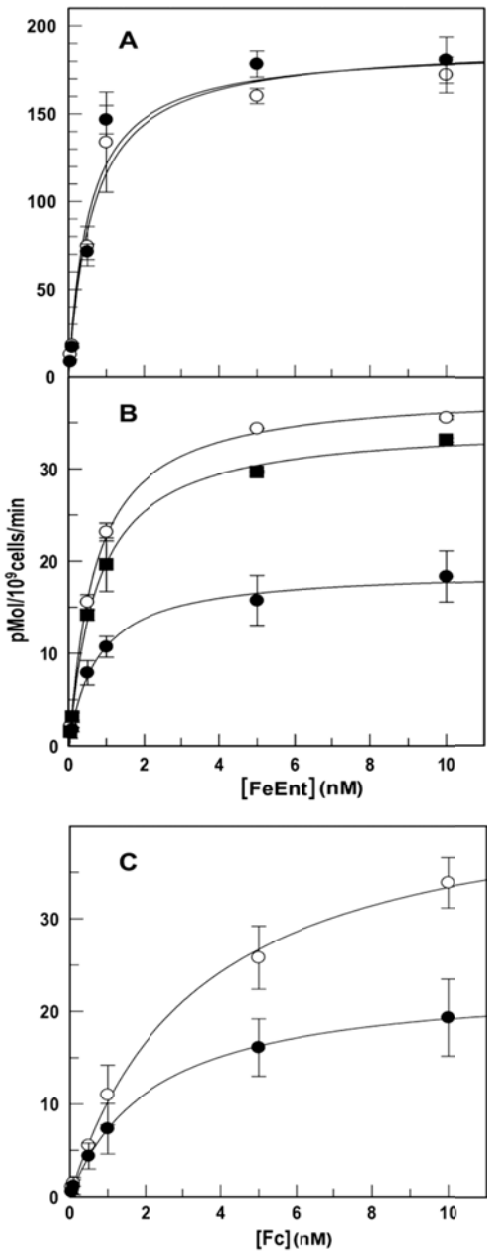

Figure 12. FeEnt transport in the presence of Fc. BN1071 was studied using standard ^{59}FeEnt uptake assays (**panel A**). The bacteria were measured for ^{59}FeEnt uptake over a range of concentrations in the absence (○) or presence (●) of 100 μM Fc. BN1071 was also subjected to PUB measurements (**panel B**). The cells were assays in normal ^{59}FeEnt binding (○), blocked (●), and PUB (■) conditions in the presence of 100 μM Fc. Standard ^{59}Fc uptake assays were done in the absence (○) or presence (●) of 100 μM FeEnt (**panel C**).

Activation energy of FeEnt transport through the OM

By studying fluorescently labeled FepAS271C, we were able to determine the activation energy of FeEnt transport through the OM. We used the Arrhenius equation to calculate the activation energy by fluorescence spectroscopic measurements of FeEnt uptake at various temperatures (49). OKN3, pFepAS271C was modified by FM and the bacteria were exposed to 10 nM FeEnt. As seen in previous studies (49), the binding and transport of FeEnt quenched fluorescence emissions and the fluorescence only recovered after FeEnt was depleted from solution. Temperature dependence of FeEnt uptake was determined in two separate ways: time required to deplete 10 nM FeEnt from solution (depletion threshold) and steady-state uptake rate at half-saturation (depletion rate) (Fig. 13). Fluorescence spectroscopic measurements were made at, 20°C, 15°C, 10°C, and 5°C. For the first method, we observed the time from the addition of FeEnt until F/F_0 increased upward to a value of 0.4. As the temperatures decreased, the times for fluorescence recovery were 200, 1630, 2600, and 6870 seconds. In the second method, we measured the rate at which fluorescence recovered by calculating the slope of the curves at half-saturation. At 20°C the slope at half saturation was 0.0023 K, at 15°C the rate was 0.00061 K, at 10 °C the rate was 0.00031 K, and at 5°C the rate was 0.00009 K. We analyzed the Arrhenius plots, ln(k) versus 1/T and the calculated values of the

activation energy were 33 (± 8) and 36 (± 5) kcal/mol of FeEnt for the depletion rate and depletion threshold methods, respectively.

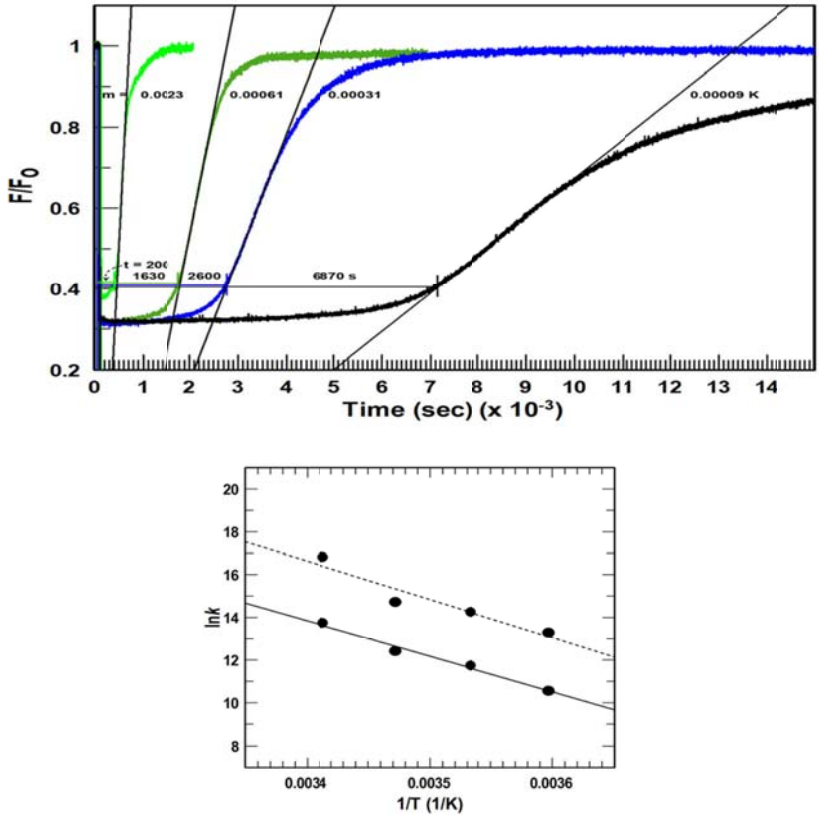

Figure 13. Activation energy of FeEnt uptake through the OM. Bacteria containing FepAS271C were labeled with FM and 10 nM FeEnt was added and the fluorescence emissions were observed at various temperatures (**top panel**). By analyzing the spectroscopic data during FeEnt uptake, we determined the activation energy of FeEnt transport through FepA. The addition of FeEnt quenched the fluorescence emissions until the siderophore was depleted from solution and the fluorescence emissions recovered. Observations were made at 20°C (green curve), 15°C (dark green curve), 10°C (blue curve), and 5°C (black curve) The time for the fluorescence to recover and the rates of recovery were used to calculate the relationship between temperature and the uptake rate (k_2). Arrhenius plots (●) were analyzed and E_a was calculated, 33 (± 8) and 36 (± 5) kcal/mol of FeEnt transported for the depletion rate (dashed lines) and depletion threshold (solid line) methods, respectively (**bottom panel**). Data obtained from previous experiments from Cao, et al. (49).

Discussion

Initially, the amount of energy required for FeEnt transport through FepA was unknown. By analyzing Arrhenius plots, we calculated the activation energy of FepA-mediated FeEnt transport, ~35 kcal/mol. This value can be interpreted as a Q_{10} temperature coefficient of 6-7 (60). Q_{10} values greater than 2 usually indicate that significant conformational change occurs during the biochemical reaction. The Q_{10} value calculated for FeEnt transport through FepA suggested that a conformational change may occur within the N-domain of FepA.

PUB assays are direct measurements of siderophore uptake through the OM. These determinations indicated that FepA could not internalize FeEnt without TonB and a proton motive force. Siderophore uptake assays and PUB determinations in the presence of multiple iron siderophores also provided information about the activity of TonB during metal uptake. Within the cell there is a limited number of TonB proteins and an abundance of TonB-dependent OM receptor proteins. Simultaneous metal uptake should affect the rate of iron transport through the OM. ^{59}Fc uptake by FhuA showed a 50% decrease in V_{max} in the presence of FeEnt. The amount of FepA is greater than FhuA in the OM, so this result was consistent during the simultaneous metal uptake of FeEnt and Fc. FeEnt uptake assays and PUB measurements showed that simultaneous transport of Fc had little effect on FeEnt uptake.

The ratio of TonB:FepA in iron-deficient conditions is 1:35 (47,52). This suggests that at any time, only 3% of all FepA proteins are actively transporting FeEnt through the OM. If only a small percentage is actively participating in FeEnt transport, than the overall rate of FeEnt uptake ~ 5 min^{-1} (39,47,48) is an underestimate and could be 30 times larger. PUB measurements showed that all FepA proteins bound with FeEnt were able to transport the ligand. This indicated that during an 80 second period, TonB was able to identify the ligand-bound receptor and interact with the OM protein and allow iron uptake. Under these circumstances, one TonB protein facilitated in the transport of approximately 20 FepA proteins. This may be the rate-limiting step in FeEnt uptake, which may explain the low turnover number.

^{59}FeEnt accumulation and PUB assays showed three uptake stages of FeEnt through FepA. The three phases were a rapid initial phase that occurred during the first 30 seconds, a secondary phase that occurred from 0.5 to 10 minute, and a steady-state rate that continued from 10 to 90 minutes. These results may reflect the involvement and interaction of the proteins involved during FeEnt uptake: TonB-ExbBD, FepB and FepCDG-Fes. If we assume that FeEnt is not associated with any proteins involved in the FeEnt uptake system, the first rate measurements begin with the initial binding of FeEnt to FepA. The second stage would be the saturation of TonB with FepA or FepB with FeEnt. During this stage FepB would be transferring FeEnt to the IM permease

complex. In the last stage, all proteins involved in the FeEnt transport system would be saturated by FeEnt or FeEnt-bound proteins.

To investigate the triphasic time course seen in the accumulation assays, PUB measurements were taken at three separate time points, 15 seconds, 5 minutes, and 25 minutes (Fig. 7). The results supported the presence of three different uptake rates. Immunoblots were done on these samples and the concentrations of FepA between the samples were similar. These results suggested that the decrease in transport rate through FepA caused the drop in overall siderophore accumulation into the cytoplasm (31). If this is true, it is possible that the OM transport activity of FepA is regulated by other cell envelope or intracellular processes.

PUB determinations with strains lacking FepB, FepD or FepG resulted similarly to the *ΔtonB* strain. Initially, the results implied that FepA could not transport FeEnt through the OM without the periplasmic binding protein or an active IM permease complex. Fluorescein maleimide was able to covalently label FepAS271C in the *ΔfepB* strain, unlike *ΔtonB* bacteria, where FM could not label FepAS271C. This indicated that in the absence of FepB, FepA was able to transport FeEnt, whereas in the absence of TonB, FepA is unable to transport FeEnt. Investigations with TolC helped elucidate the results of strains lacking the perisplasmic protein or IM permease proteins where retention of FeEnt and transport through FepA seemed impaired. We conducted PUB and siderophore

retention measurements that showed TolC was responsible for the export of FeEnt. In the absence of FepB or the IM permease proteins, FeEnt accumulates within the periplasmic space and is unable to be transported into the cytoplasm. The accumulation results in an export of the excess FeEnt by TolC. This futile cycle stresses the importance of the periplasmic binding protein and an active inner membrane permease complex.

Chapter 4: Determining conformational change in FepA during FeEnt uptake through FRET analysis

Background

The N-domain of FepA occludes the FepA channel and has low affinity for the ligand (61). This occlusion of the C-domain leaves no space for FeEnt to pass through FepA during iron uptake and the N-domain of FepA must undergo a conformational change to allow the ligand to enter the periplasmic space.

Two possible models have been discussed that could allow FeEnt transport through FepA by conformational rearrangements of the N-domain (25,38,53). In the first model, which will be referred to as the ball-and-chain model, the entire N-domain is ejected from the barrel in a concerted movement. Once the N-domain is dislodged into the periplasm, the FeEnt can pass through the OM channel. In the second model, transient pore model, the N-domain would rearrange within the FepA barrel producing a narrow passage way for FeEnt. We constructed double Cys substituted mutants in FepA and conjugated these sites with Cys specific fluorophores to try and determine the model of FeEnt transport through FepA.

Experimental Procedures

Construction of double cysteine substitution mutants in FepA

Double cysteine mutants in FepA were first constructed by engineering single cysteine mutations in *fepA* on pITS23 or pITS47. The

single Cys substitutions were constructed based on the method in chapter 2. The location of the single Cys substitutions were based on previous fluorescent spectroscopy data (38,40) and the location of the residues. To determine conformational change within the N-domain of FepA, one Cys substituted mutant must be located on the extracellular loops of FepA and the other must be located on the periplasmic surface of the N-domain of FepA. Once the single Cys substitutions were made in FepA, we constructed double cysteine mutants by restriction fragment exchange with the endonucleases PstI and MluI. Cysteine substitutions were verified by DNA sequence analysis. Unless stated otherwise, all plasmids were harbored in OKN3 strains.

Fluorescence labeling of FepA Cys sites *in vivo* for FRET analysis

FRET is the radiationless energy transfer between two molecules, a donor (the excited fluorophore) and an acceptor (a fluorophore or chromophore). The excited donor molecule transfers energy by resonance and induces excitation of the acceptor electrons. The de-excitation of the acceptor molecule mainly results in a photon emission. The energy transfer efficiency is dependent upon three conditions: the spectral overlap between the emission spectrum of the donor fluor and the excitation spectrum of the acceptor fluor, the distance between the fluorophores, and the orientation of their dipoles (62). The energy transfer efficiency between the fluors can be used to calculate the distance between the fluorophores.

We used fluorescein maleimide as the donor fluorophore and Alexa Fluor 546 maleimide, A546M, as the acceptor fluorophore. Fluorescein maleimide has an excitation maximum at ~493 nm and an emission maximum at ~520 nm. Alexa Fluor 546 maleimide has an excitation maximum at ~554 nm and an emission maximum at ~570 nm. These fluorescent dyes were ideal because of their spectral overlap (Fig. 14) and their relative sizes. The molecular weight of FM is 427 Da and the molecular weight of A546M is 1034 Da.

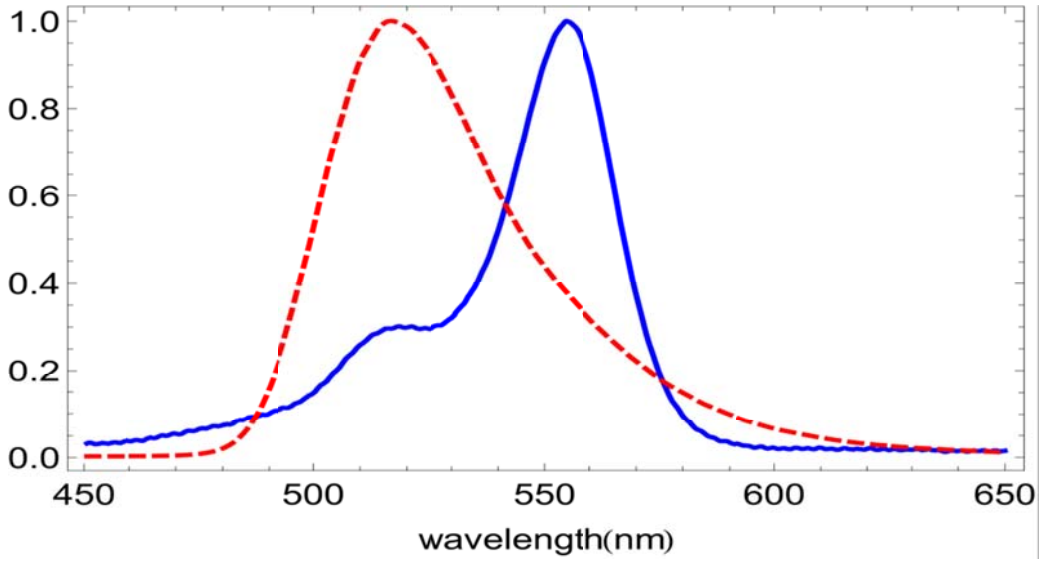

Figure 14. Spectral overlap of FM and A546M. The normalized emission spectra and excitation spectra of the FRET pair FM and A546M, respectively. The red dashed line represents the emission spectra of FM with an emission maximum at ~520 nm. The blue solid line represents the excitation spectra of A546M with an excitation maximum at ~554 nm.

The size exclusion limit of the OM porins is 650 Da (20). This means that FM can traverse the OM through the porins and covalently label any Cys residues that are exposed to the periplasmic space (38). A546M will be limited to labeling any Cys residues on the extracellular surface.

By fluorescently labeling the double Cys substituted mutants in FepA with A546M initially, the extracellular Cys residue is labeled and the remaining Cys mutant exposed to the periplasmic space is unmodified. To covalently modify the N-domain Cys mutant, we introduced FM at a high concentration to ensure enough FM will be able to traverse the OM porins and conjugate with the Cys mutant on the periplasmic surface of FepA.

This procedure is a modified version of the fluorescence labeling procedure listed in chapter 2. Cells were subcultured in MOPS minimal media and allowed to grow for 5.5 hours or until late log phase. We measured the OD_{600} and 5 x 10^8 cells were collected by centrifugation at 17,000xg for 1 minute at 4°C. The cells were then washed and resuspended in 1 mL of 50 mM Na_2HPO_4, pH 6.5, 0.9% NaCl, containing 0.4% glucose. We incubated the cells for 10 minutes at 37°C. Alexa Fluor 546 maleimide, A546M, was added to the cells (5 to 25 μM) first before the addition of FM. Once AM was added, the cells were incubated at 37°C for 15 minutes. Then, we introduced FM to the cells at 300 μM and the cells were incubated for an additional 15 minutes at 37°C. At the end of the labeling period, the reactions were quenched and the cells were

washed three times. For spectrophotometric studies, we resuspended the cells in 1 mL TBS (50 mM Tris chloride, pH 7.4, 0.9% NaCl), 0.4% glucose. For detection of fluorescence labeling by SDS-PAGE, 1 x 10^8 bacteria was lysed by boiling for 5 minutes in SDS-PAGE sample buffer before resolution by SDS-PAGE.

Fluorescence spectrophotometry

Spectrofluorometric studies were carried out using an SLM-AMINCO 8000 fluorometer, upgraded to 8100 functionality. After the cells were labeled with FM and/or A546M, we conducted an emission scan (510 – 580 nm) with an excitation of 488 nm at various temperatures. We chose the excitation wavelength of 488 nm to maximize the excitation of FM and minimize the direct excitation of A546M. The emissions at 520 nm and 573 nm were the values of interest providing information on the fluorescence of FM and A546M, respectively. The results of the emission scan would provide information on the energy transfer and therefore the distance between the dyes. To provide additional information on the energy transfer and fluorescence of the dyes, we also conducted an excitation scan (450 – 565 nm) with an emission of 570 nm at various temperatures. The amount of cells measured in the experiments varied depending on the slit width used during each experiment.

Results

Double Cys substituted mutants in FepA

Energy transfer between the fluorophores can occur from 10 to 100 Å. The Förster distance, R_0 (Å), is the distance at which the energy-transfer efficiency is 50%. The estimated Förster distance of fluorescein maleimide and Alexa Fluor 546 maleimide is 60 Å. This estimation was based on using 0.79 as the quantum yield of fluorescein (63). We constructed double Cys substituted mutants in FepA in a way to satisfy these parameters and to allow for interpretation of conformational change in the N-domain during FeEnt transport.

Based on previous experiments (38,40), surface residues S271C, E280C, and A698C of FepA were chosen as suitable sites for biochemical analyses. In addition to these residues, we engineered A261C and S275C of FepA based on their location in FepA. These residues are located on the mobile surface loops and are on the “hinge-side” of FepA, where the globular N-domain is connected to the β-barrel C-domain. It is likely that the N-domain of FepA forms a pore opposite of the “hinge” where the N-domain and the C-domain are connected during FeEnt transport. If this does occur, determining the distance between the dyes conjugated to the Cys substitutions in FepA during FeEnt transport could help differentiate between the models of iron transport through FepA (Fig. 15). Cys substitutions on the short immobile surface loops of FepA were also engineered, K167C and V438C. These sites could be more beneficial

when interpreting conformational change within the N-domain using FRET. Preliminary fluorescent labeling experiments with K167C and V438C revealed these residues were inaccessible to modification by A546M and therefore, we dismissed these residues for double Cys substituted mutants in FepA (data not shown). On the periplasmic surface of the N-domain of FepA, residues L23C, T30C, and A33C were of interest. Based on these residues of interest, we constructed the double mutants L23C/A261C, L23C/S275C, T30C/S271C, T30C/E280C, A33C/E280C, and A33C/A698C in FepA (Table 3).

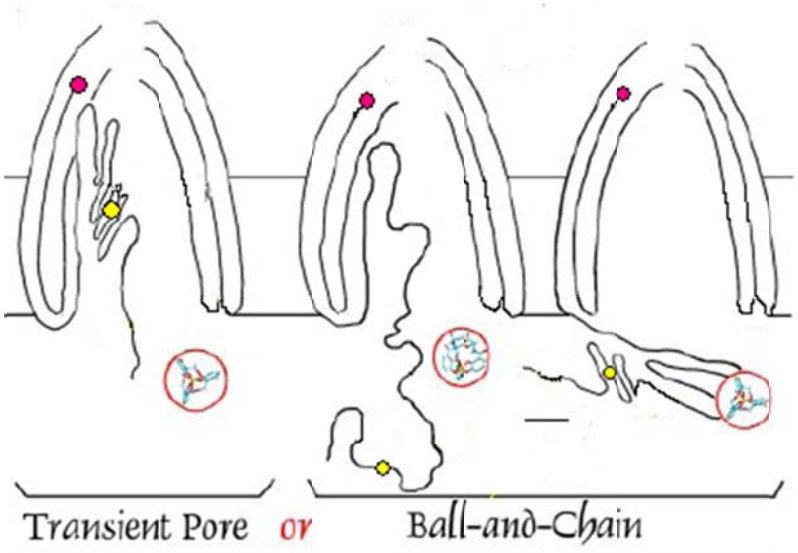

Figure 15. Graphical representation of the transient pore and ball-and-chain model of FepA conjugated to A546M and FM. This figure was adapted from Ma, et al. (38). FeEnt is shown within the red circle. An extracellular residue labeled with A546M is shown as a pink circle and the N-domain residue labeled with FM is shown as a yellow circle. We would calculate the distance between the dyes prior to FeEnt transport and would determine the model of transport through FepA once we introduced FeEnt. In the transient pore model the distance between the residues would decrease and in the ball-and-chain model the distance between the residues would increase.

Table 3. Double Cys substituted mutants in FepA for FRET analysis

Double Cys mutant in FepA	Distance between α-carbons (Å)
L23C/A261C	40.0
L23C/S275C	49.3
T30C/S271C	46.3
T30C/E280C	35.1
A33C/E280C	32.1
A33C/A698C	55.2

As mentioned earlier, the locations and the distances between the residues are important to the study for FRET analysis. The distances between the residues of all the double Cys mutant derivatives of FepA are within the Förster distance (Table 3) and should have greater than 50% energy transfer efficiency. This is paramount to the interpretation of the results in the absence and presence of FeEnt. Measurements of the distance between the dyes could help determine the model of FeEnt transport through FepA. For example, based on the crystal structure of FepA, the distance between the residues T30C and S271C in the double Cys mutant in FepA in the absence of FeEnt should be 46.8 Å (25). During FeEnt transport the distance between the dyes could increase or decrease based on the model of FeEnt transport through FepA (Fig. 15). If the distance between the residues increases, it would suggest that the N-domain of FepA was dislodged into the periplasm. If the distance between

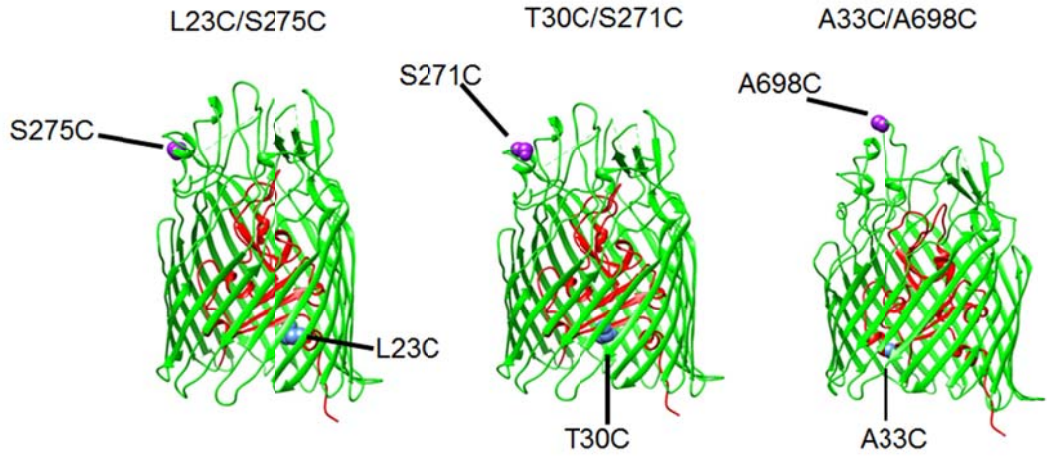

Figure 16. Graphical representation of the double Cys substituted mutants in FepA for FRET analysis.

the residues decreases, it would imply the N-domain remained in the β-barrel of FepA.

Based on the results when optimizing fluorescence labeling *in vivo*, any double Cys substituted mutants containing residues A261C and E280C were removed. The double Cys substituted mutants in FepA L23C/S275C, T30C/S271C, and A33C/A698C were used for FRET analysis (Fig. 16).

Effect of Cys substitution(s) and fluoresceination of FepA during FeEnt uptake

The effect of the Cys substitution(s) and covalent modification on FepA during FeEnt uptake must be considered. We conducted preliminary siderophore nutrition tests to compare the growth of Cys substituted FepA to wild-type FepA. This assay was a qualitative assay that indicated if the

Cys mutant derivatives of FepA functioned like the wild-type protein. We conducted siderophore nutrition assays on the wild type (OKN3/pITS47), the single Cys substituted FepA derivatives, the double Cys substituted FepA mutants, and OKN3 (*ΔfepA*) (Fig. 17). In the siderophore nutrition tests, all of the Cys mutant derivatives of FepA transported FeEnt similar to wild-type FepA.

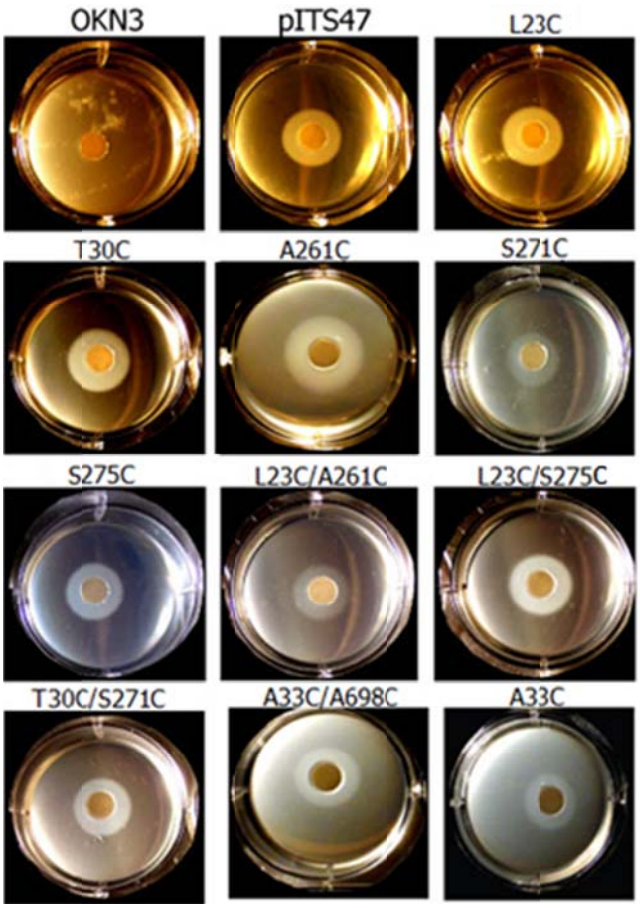

Figure 17. Siderophore nutrition tests of Cys substituted mutant(s) in FepA. Bacterial cultures were plated in LB media containing 233 μM bipyridyl. We placed a paper disc in the center of the agar and 0.5 nmol of FeEnt was added to the center of the disc. The zones of bacterial growth (halo) of the Cys substituted mutants were compared to wild-type pITS47 and it was determined the mutants could transfer FeEnt like wild-type FepA. The Cys substituted mutation A698C is not shown in the figure but has been assayed before and transported FeEnt like wild-type FepA (38).

To determine the effects of FeEnt uptake by Cys substitution(s) in FepA and/or covalent modification by fluorophores, we also conducted a modified version of siderophore uptake and binding assays. ^{59}FeEnt transport was determined by collecting data at two times: 5 seconds and 25 seconds. Bacteria were grown in MOPS minimal media and the samples were labeled with FM and/or A546M. An aliquot was allowed to incubate in a 37°C water bath. The cells were then mixed with 10 mL MOPS containing 10 nM ^{59}FeEnt. Incubation was allowed at the various time points 5 seconds and 25 seconds and the cells were then collected on filters and rinsed. By calculating the difference of the counts at two separate time points and extrapolating the 20 second transport, we determined the uptake of ^{59}FeEnt in one minute. A bar graph of pmol ^{59}FeEnt/10^9 cells/minute versus the sample was used to determine the effects of the Cys substitution(s) in FepA and the covalent modification by FM and/or A546M. FeEnt uptake and binding experiments have been conducted on A33C/A698C and T30C/S271C using pITS23 and pITS47, as the wild-type strain, respectively (Fig.18).

The siderophore binding and uptake assays indicated that the double Cys mutation A33C/A698C in FepA had lower FeEnt transport than wild-type pITS23. This was also seen when the fluorophores were conjugated to the double Cys mutants in FepA. A possible explanation for this impairment may be due to the fluorophores inhibiting the transport of FeEnt through FepA. It is also possible that the double Cys mutants that

have been covalently modified by the fluors have a slower rate of transport than wild-type FepA. When comparing the double mutant T30C/S271C in FepA to wild-type pITS47, the transport was unaffected by the Cys substitutions in FepA. The FeEnt transport was also unaffected when the fluorophores were conjugated to the double Cys T30C/S271C mutants in FepA.

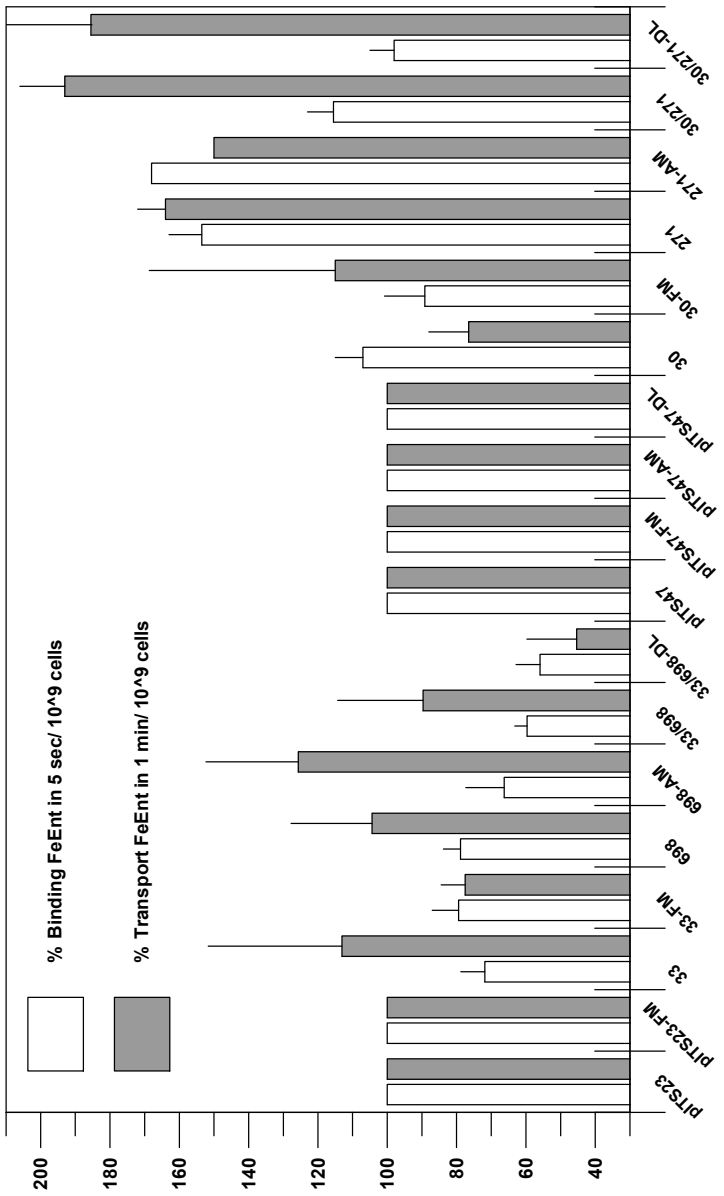

Figure 18. FeEnt binding and uptake of Cys substituted mutant(s) in FepA covalently modified by fluorophores. Bacteria were subcultured in MOPS minimal media and subjected to fluorescence labeling with 5 μM (A33C/A698C and A698C) or 15 μM A546M (T30C/S271C and S271C) and/or 300 μM FM. ^{59}FeEnt uptake assays were conducted at two separate time points. The results were shown as the percent of FeEnt binding in 5 seconds and percent of FeEnt transport through FepA in 1 minute (percentage was compared to wild-type FepA (100%)) in the absence and presence of the fluorophores.

Optimizing fluorescent labeling in vivo

The double mutants that were constructed in FepA were L23C/A261C, L23C/S275C, T30C/S271C, T30C/E280C, A33C/E280C, and A33C/A698C. To determine optimal labeling conditions with A546M and FM, we conducted labeling experiments with all of the single Cys mutant derivatives of FepA. The extracellular residues located on the loops of FepA were labeled with varying concentrations of A546M. The residues located on the periplasmic surface of the N-domain of FepA were labeled with varying concentrations of FM.

FepA residue E280C showed minimal covalent modification in comparison with S271C (data not shown). To improve A546M labeling of FepAE280C, we introduced pFepAE280C in CL29 (42) by electroporation. This host strain has a truncated lipopolysaccharide (LPS) core. By using a deep rough strain, it was possible the residue E280C in FepA would be more accessible to the fluorophore. CL29/pFepAE280C did not improve accessibility to the modification by A546M (Fig. 19). The expression of FepA was also greatly decreased in the strain. Due to these results, we excluded the double mutants T30C/E280C and A33C/E280C in FepA for FRET analyses.

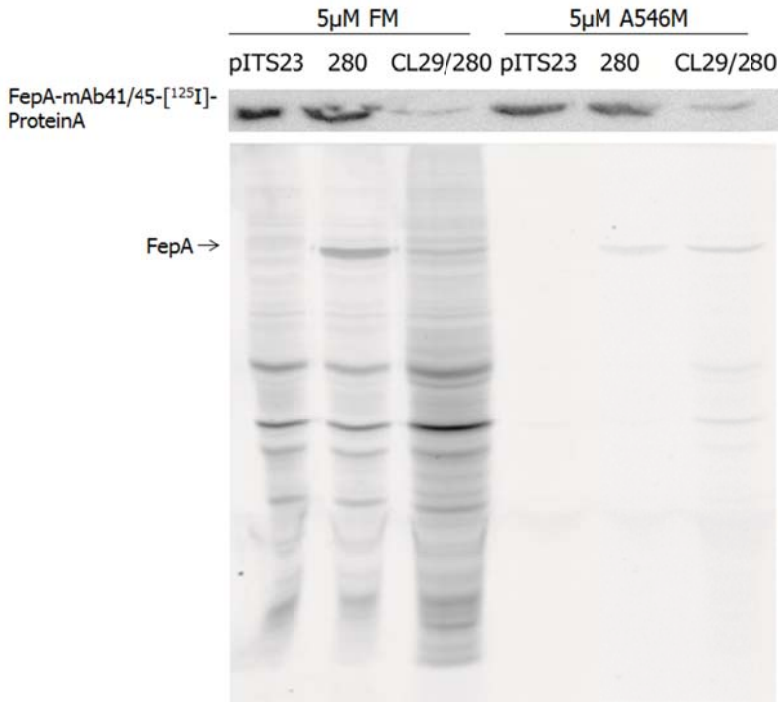

Figure 19. SDS-PAGE and immunoblot of pFepA280C. To determine the extent of fluorescent labeling of pFepAE280C in CL29 (rough strain) and OKN3 (*ΔfepA*), we labeled cells with 5μM FM or 5μM A546M at 37°C and the cells incubated for 15 minutes. After fluor labeling the samples were analyzed through SDS-PAGE and visualized by a StormScanner (**bottom lanes**). To compare the FepA expression in all of the strains, the proteins in the gel were transferred to nitrocellulose, incubated with anti-FepA mAb 41/45, [^{125}I]-protein A and scanned on a phosphorimager (**top lanes**). pITS47 harbored in OKN3 was not modified by FM or A546M because the two native Cys are in a disulfide bond.

We labeled the remaining extracellular Cys mutant derivatives of FepA A261C, S271C, S275C, and A698C with various concentrations of A546M. The Cys substituted mutant A261C in FepA had little to no modification by A546M (data not shown) with concentrations as high as 30 μM A546M. FepA derivatives S271C, S275C, and A698C were all accessible to A546M and were conjugated to the fluor to the same extent.

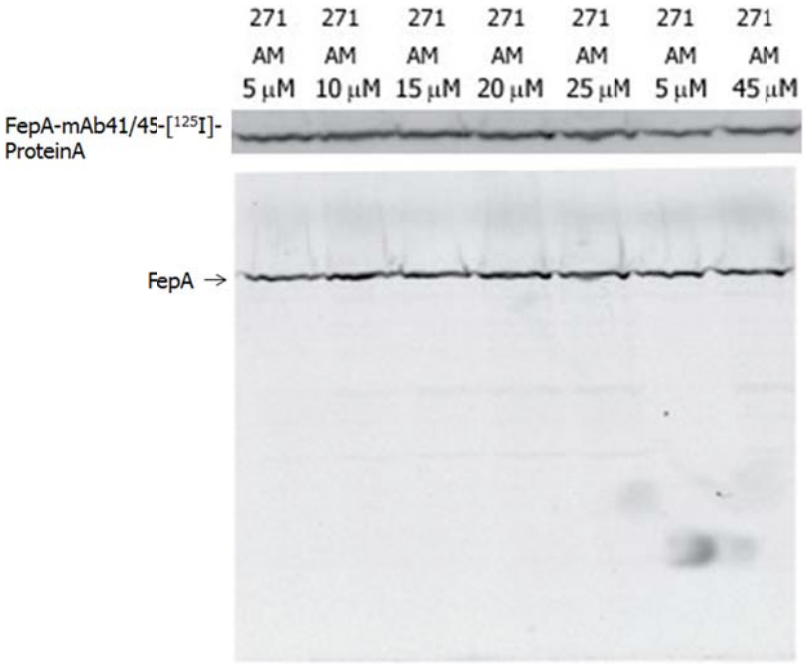

Figure 20. SDS-PAGE and immunoblot of pFepAS271C. To determine the extent of fluorescent labeling of pFepAS271C, we labeled the cells with 5, 10, 15, 20, 25, and 45 μM A546M at 37°C and incubated the cells for 15 minutes. After fluor labeling the samples were analyzed through SDS-PAGE and visualized by a StormScanner (**bottom lanes**). To compare the FepA expression in all of the samples, we transferred the proteins to nitrocellulose, incubated the blot with anti-FepA mAb 41/45, [^{125}I]-protein A, and scanned the blot on a phosphorimager (**top lanes**). The fluorescence labeling of S271C in FepA did not significantly increase with increasing concentration of A546M. This image has been altered to improve the visibility of FepA.

Figure 20 is representative of the extent of A546M modification of the Cys substituted mutants in FepA.

We subjected the Cys mutants located in the N-domain of FepA L23C, T30C, and A33C to fluorescent labeling experiments with varying concentration of FM. The FepA derivative L23C was the most accessible to FM; the remaining FepA Cys mutants T30C and A33C were also covalently modified by FM (Fig. 21). An increase of FM concentration

during fluorescent labeling increased the conjugation of FM to the Cys mutants located in the N-domain of FepA. To determine if labeling times and temperatures could be optimized to modify the Cys of interest and minimize background fluorescence labeling by FM, we conducted an additional labeling experiment on the FepA derivative L23C (data not shown). Based on both of the labeling results, we used 300 μM FM and incubated at 37°C for 15 minutes during all *in vivo* fluorescent labeling experiments.

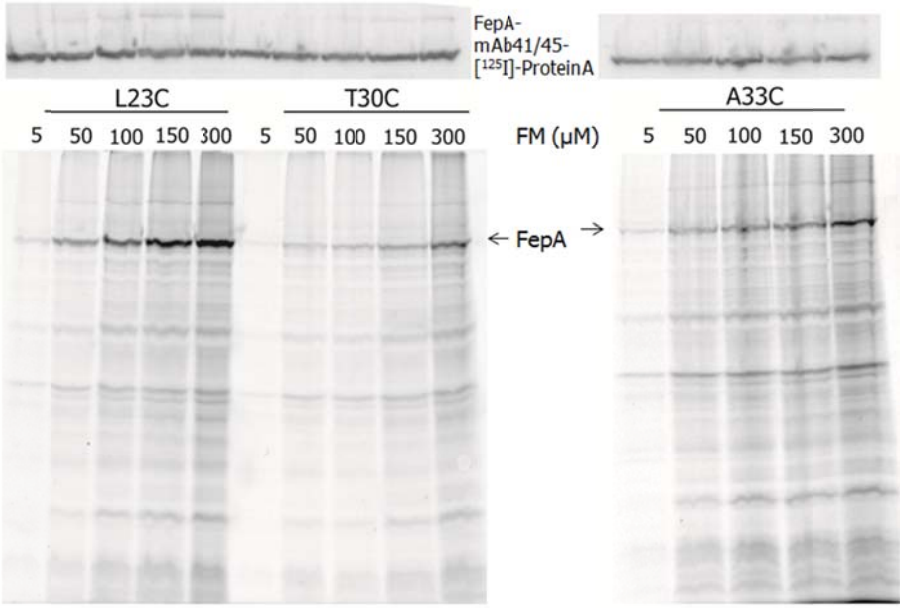

Figure 21. SDS-PAGE and immunoblot of pFepAL23C, pFepAT30C, and pFepAA33C. To determine the extent of fluorescent labeling of the Cys substituted mutants L23C, T30C, and A33C in FepA, we labeled the cells with 5, 50, 100, 150, and 300 μM FM at 37°C and the cells incubated for 15 minutes. After labeling, we analyzed the samples through SDS-PAGE and visualized it by a StormScanner (**bottom lanes**). To compare the FepA expression in the samples, the proteins were transferred, incubated with anti-FepA mAb 41/45, [^{125}I]-protein A and scanned on a phosphorimager (**top lanes**). The fluorescence labeling of all the N-domain Cys substituted mutants in FepA increased with increasing concentration of FM.

Spectrofluorometer study of FRET

As discussed earlier the energy transfer, *E*, of the donor and acceptor molecules can be used to determine the distance between the dyes, *r*, if the Förster distance, R_0, of the dyes is known. The equation below shows this relation and how dependent the energy transfer efficiency is on the distance of the donor and acceptor dyes. Measurements of *r* are only reliable if the distance of the dyes is within $2R_0$.

$$E = \frac{R_0^6}{R_0^6 + r^6}$$

The energy transfer, *E*, is calculated by determining the fluorescence intensities of the donor dye in the absence (F_D) and presence of the acceptor molecule (F_{DA}).

$$E = 1 - \frac{F_{DA}}{F_D}$$

To determine the fluorescence intensities of the FM in the absence and presence of A546M, we conducted emission scans with an excitation of 488 nm. The emission was scanned from 510 to 580 nm. This would allow the determination of the FM fluorescence emission at 520 nm and the fluorescence emissions of A546M at ~573 nm. In the absence of FeEnt, the fluorescence intensity of FM should decrease in the presence of A546M and the fluorescence intensity of A546M should be seen at ~573 nm.

In addition to the emission scan, we conducted an excitation scan (450 – 565 nm) with an emission of 570 nm. This information was not used to determine the distance between the dyes but was used as a qualitative assay. In the excitation scan, a fluorescence intensity at 490 nm should only show when both FM and A546M were present. This would also indicate that energy transfer between the two dyes occurred.

To appropriately analyze the spectroscopic data, we considered controls to account for covalent modification of other proteins during *in vivo* labeling experiments. FepA does not contain any free sulfhydryl groups for covalent modification but it has been shown that other proteins are modified by thiol specific fluors (38,40). To determine the background fluorescence that was not attributed by FepA, we conducted spectroscopic experiments with pITS47 labeled with FM and/or A546M (Fig. 22 and 23).

The results of the pITS47 labeling experiment showed FM and/or A546M labeled the bacterial cells at a low level and the excitation and emission scans displayed low levels of fluorescence intensity. These values were compared to the Cys mutant derivatives of FepA that were initially tested T30C, S271C, and T30C/S271C.

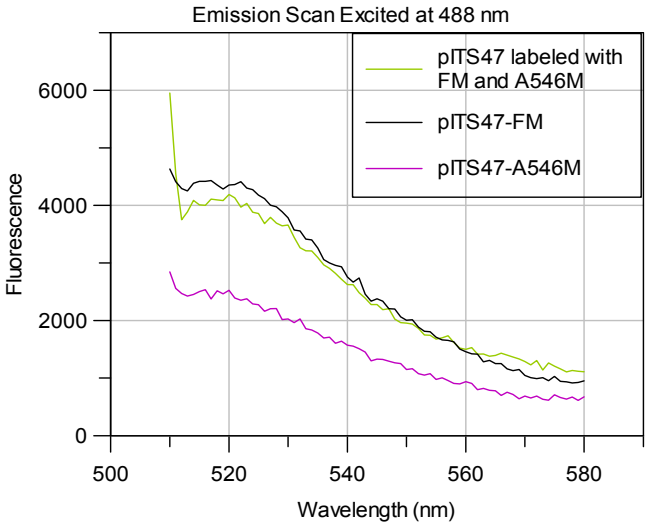

Figure 22. Emission scan of pITS47 labeled with FM and/or A546M. OKN3 cells harboring pITS47 were subjected to fluorescence labeling with 17 μM A546M (purple) or 300 μM FM (black) or both fluors (green). We analyzed 9 x 10^6 cells in a spectrofluorometer. An emission scan was conducted with an excitation at 488 nm. In comparison to the Cys derivatives of FepA, fluorescence intensities were relatively low.

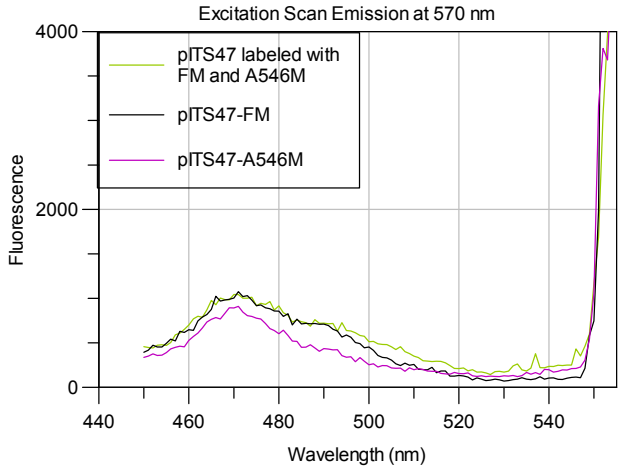

Figure 23. Excitation scan of pITS47 labeled with FM and/or A546M. OKN3 cells harboring pITS47 were subjected to fluorescence labeling with 17 μM A546M (purple) or 300 μM FM (black) or both fluors (green). We analyzed 9 x 10^6 cells in a spectrofluorometer. An excitation scan was conducted with an emission at 570 nm. In comparison to the Cys derivatives of FepA, fluorescence intensities were relatively low.

The Cys mutant derivatives of FepA T30C, S271C, and T30C/S271C were subjected to the same fluorescent labeling conditions and spectroscopy scans. To calculate the corrected fluorescence intensities of the Cys mutants of FepA (Fig. 24 and 25), we subtracted by the fluorescence intensities of the wild-type, pITS47.

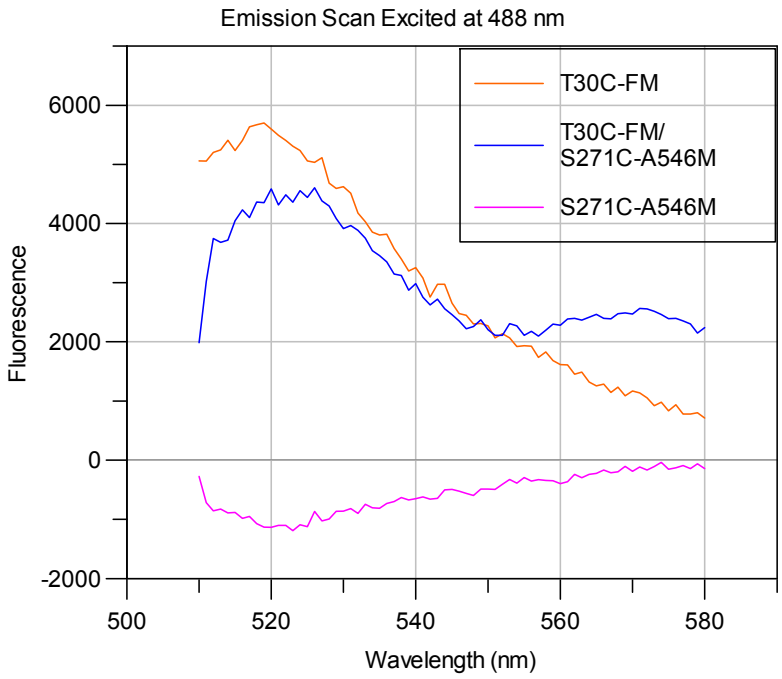

Figure 24. Corrected emission scan of FepA mutants T30C, S271C, and T30C/S271C conjugated to the appropriate fluors. The bacterial cells were fluorescently labeled *in vivo* with 17 μM A546M and/or 300 μM FM. The FepA derivative T30C (orange) was labeled with 300 μM FM. The Cys substituted mutant S271C (pink) in FepA was covalently modified with 17 μM A546M. The double Cys mutant in FepA T30C/S271C (blue) was labeled with 17 μM A546M initially and then 300 μM FM. We analyzed 9 x 10^6 cells in a spectrofluorometer. An emission scan was conducted with an excitation at 488 nm. The fluorescence intensity values were subtracted by the fluorescence values of pITS47 labeled with the appropriate fluor. The fluorescence intensities of T30C-FM and T30C-FM/S271C-A546M differ at 520 nm and 570 nm, this suggested energy transfer occurred between the donor and the acceptor dyes.

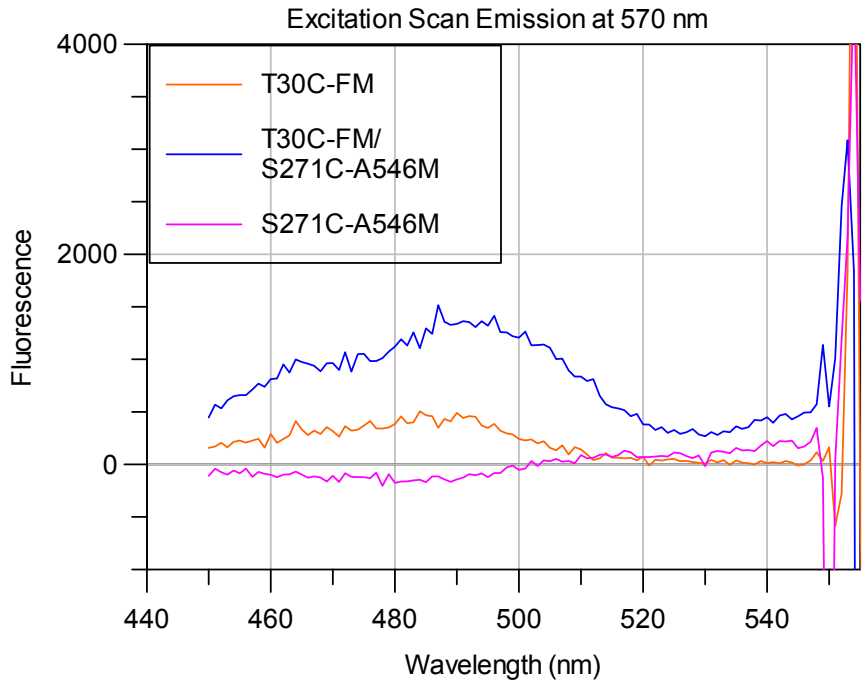

Figure 25. Corrected excitation scan of FepA mutants T30C, S271C, and T30C/S271C conjugated to the appropriate fluors. The FepA derivative T30C (orange) was labeled with 300 μM FM. The Cys substituted mutant S271C (pink) in FepA was covalently modified with 17 μM A546M. The double Cys mutant in FepA T30C/S271C (blue) was labeled with 17 μM A546M initially and then 300 μM FM. We analyzed 9 x 10^6 cells in a Spectrofluorometer and conducted an excitation scan with an emission at 570 nm. The fluorescence intensity values were subtracted by the fluorescence values of pITS47 labeled with the appropriate fluor. The fluorescence intensities of T30C-FM and T30C-FM/S271C-A546M differ at ~490 nm, this suggested that energy transfer occurred between FM and A546M.

The results of the corrected emission and excitation scans, suggested that energy transfer between FM and A546M occurred. In the emission scan of the single Cys substituted mutant T30C in FepA, the fluorescence intensity was seen at 520 nm as expected when excited at 488 nm and the fluorescence intensity at 570 nm was relatively low. When FM was in the presence of A546M, T30C-FM/S271C-A546M, the

fluorescence intensity at 520 nm decreased and the intensity increased at 570 nm. We also conducted an emission scan on the Cys mutant S271C in FepA, the results showed that S271C-A546M did not contribute to any of the fluorescence intensities shown in the double Cys FepA mutant T30C/S271C. The excitation scan with an emission at 570 nm supported the results observed in the emission scan. Based on the emission scan results, we calculated the distance between the dyes, ~77 Å. This value was higher than expected but this could be due to the scans being conducted at 23°C, which allowed the proteins to be more mobile (64). The acceptor dye was located on a mobile surface loop so it could be reasonable that the value was higher than the expected ~47 Å.

After the spectroscopic scans of the bacteria, we analyzed the samples by SDS-PAGE and the expression of FepA was determined by an anti-FepA immunoblot (Fig. 26). The expression of FepA was similar in all single Cys mutant derivatives of FepA. The results of the immunoblot showed that the double Cys mutant in FepA T30C/S271C had an additional FepA band below the expected protein band. This band was unexpected because the SDS-PAGE analysis was done in the presence of ~160 mM βME. This suggested the additional band could not be due to an aberrant disulfide bond formation. The additional band may be a degradation product of FepA, but the source of this band remains unknown. By comparing the results of the anti-FepA immunoblot and the SDS-PAGE gel, the second band did not appear to be fluorescently labeled by FM or A546M. This was

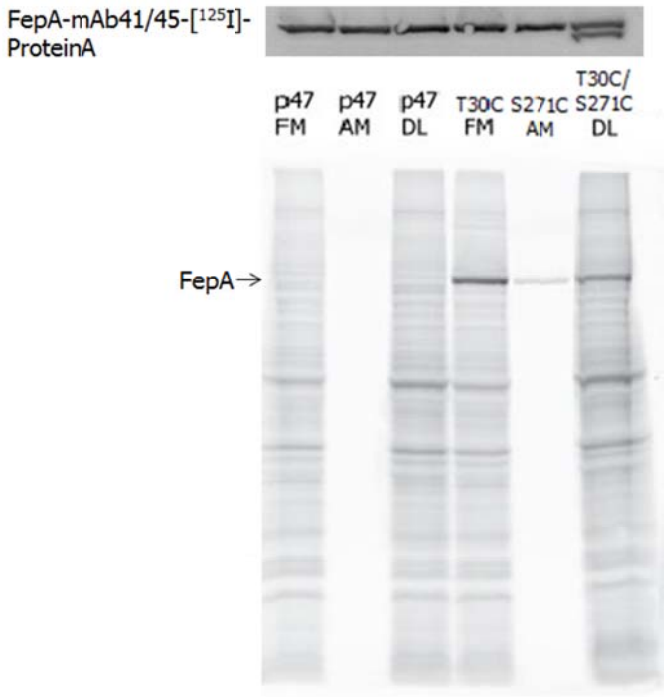

Figure 26. SDS-PAGE and immunoblot of Cys mutants in FepA. To observe the extent of fluorescent labeling of the Cys substituted mutants T30C, S271C, and T30C/S271C in FepA, we analyzed the cells through SDS-PAGE and the results were visualized by a StormScanner (**bottom lanes**). To compare the FepA expression in the samples, the proteins were transferred, incubated with anti-FepA mAb 41/45, [^{125}I]-protein A and scanned on a phosphorimager (**top lanes**). The single Cys mutant derivatives of FepA had similar expression to the wild-type parent protein.

an indication that the results of the emission or excitation scans would be unaffected by the unknown FepA band.

Several spectroscopy scans were conducted on the single and double Cys mutants of FepA T30C/S271C. Only a few experiments supported the results shown in Fig. 24 and 25. This proved problematic during the trouble shooting process of the study. The results first indicated that energy transfer could be seen between FM and A546M, but with more repetition and slight variations the results could not be duplicated. Several

adjustments were made to determine the source of error or possible sources of improvement: slit width, amount of cells present in the sample, varying the concentration of A546M present during labeling, and changing the temperature during the scans from 23°C to 4°C. We also tested the other single and double Cys mutants in FepA L23C/S275C and A33C/A698C but none of the double mutants showed an energy transfer between the two fluors that was seen with T30C/S271C.

The results of the emission scan with an excitation at 488 nm of the double Cys mutant in FepA consistently showed higher fluorescence intensity at 520 nm than the single Cys mutant in FepA conjugated to FM alone. The SDS-PAGE gel analysis would confirm this problem and at various times had a higher background than the wild-type control, pITS47. At one point, the control samples with OKN3 harboring pITS47 showed similar fluorescence intensities compared to its FepA Cys mutant equivalent, which made it impossible to interpret the data from the scans. Initially, this appeared to be a pipetting error during fluorescence labeling or during the scans. It was important to have the same number of cells during the scans so the data could be compared to one another. Adjustments were made with the pipettes and spectrofluorometer but the problems still persisted.

Despite the null results seen in the absence of FeEnt, we conducted a few emission and excitation scans in the presence of FeEnt to determine if any energy transfer could be seen during iron transport

through FepA. These experiments were conducted both at 23°C (Fig. 27 and 28) and 4°C (data not shown). At 23°C the FepA can bind FeEnt and transport at a slower rate compared to 37°C. At 4°C FepA can bind FeEnt and the uptake of FeEnt would not be able to occur during the scan.

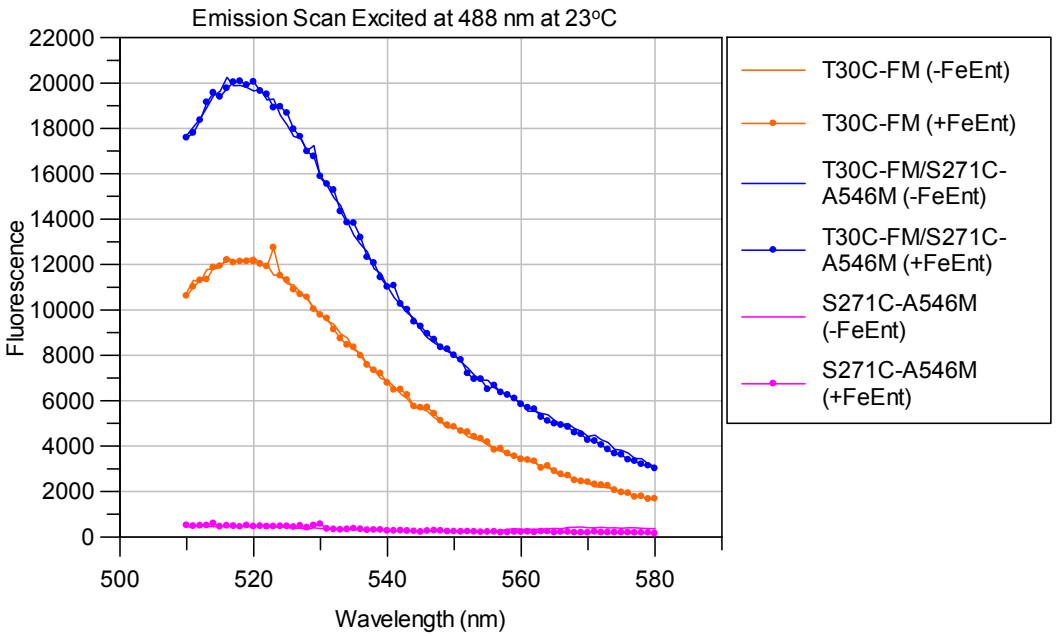

Figure 27. Emission scan of FepA mutants T30C, S271C, and T30C/S271C conjugated to the appropriate fluors in the absence and presence of 50 nM FeEnt. The FepA derivative T30C (orange) was labeled with 300 μM FM. The Cys substituted mutant S271C (pink) in FepA was covalently modified with 15 μM A546M. The double Cys mutant in FepA T30C/S271C (blue) was labeled with 15 μM A546M initially and then 300 μM FM. We analyzed 2 x 10^7 cells in a spectrofluorometer in the absence (solid line) or presence (lines with filled in circles) of 50 nM FeEnt. An emission scan was conducted with an excitation at 488 nm. The spectral data were unchanged in the presence of FeEnt.

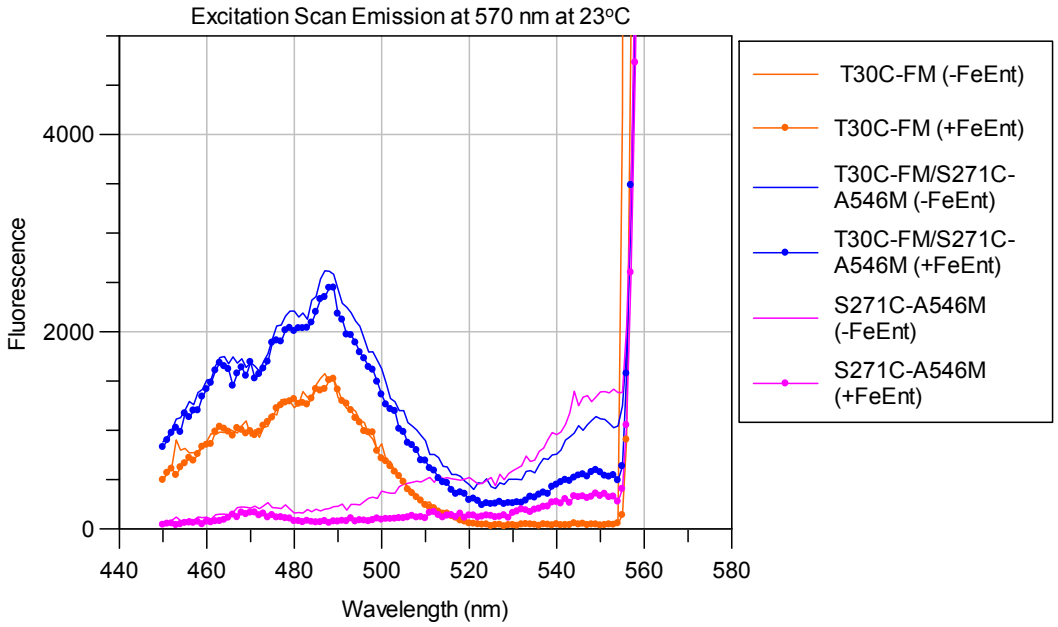

Figure 28. Excitation scan of FepA mutants T30C, S271C, and T30C/S271C conjugated to the appropriate fluors in the absence and presence of 50 nM FeEnt. The FepA derivative T30C (orange) was labeled with 300 μM FM. The Cys substituted mutant S271C (pink) in FepA was covalently modified with 15 μM A546M. The double Cys mutant in FepA T30C/S271C (blue) was labeled with 15 μM A546M initially and then 300 μM FM. We analyzed 2 x 10^7 cells in a spectrofluorometer in the absence (solid line) or presence (lines with filled in circles) of 50 nM FeEnt. An excitation scan was conducted with an emission at 570 nm. The spectral data at 490 nm appeared to be unchanged in the presence of FeEnt.

In the presence of 50 nM FeEnt, the spectral data collected from the emission and excitation scans were nearly identical to the data obtained in the absence of FeEnt. This was also seen in the scans conducted at 4°C. These results were unexpected since previous experiments indicated a conformation change within the surface loops of FepA during FeEnt transport (49,64). Fig. 27 and 28 were representative of the results seen in different double Cys mutants in FepA. This could be

an indication of the limitation of this scanning method during FeEnt transport.

Extensive studies have been conducted to determine loop conformational motion during FeEnt uptake by covalent modification by FM (65). Various Cys substituted mutants were located on the surface loops of FepA. These cells were then subjected to FM labeling and spectroscopic measurements were done to determine the extent of quenching during FeEnt transport (49). The results indicated that the surface loops of FepA could be separated into two groups characterized by the extent of quenching and recovery rates. This provided information concerning the individual loop motion during FeEnt uptake and binding. Group A (loops 2, 3 and 11) exhibited a larger extent of quenching than group B (loops 4, 5, and 8).

The double Cys mutants in FepA that were constructed for the purposes of FRET analyses have residues located in loop 3 (residues S271C and S275C) and loop 11 (A698C). Although previous studies with S271C had indicated that the loop underwent conformational change during FeEnt transport through FepA that resulted in FM quenching, we constructed double Cys substituted mutants in FepA with this extracellular residue because of the extent of labeling with A546M. These double Cys mutants in FepA were ideal for FRET analysis in the absence of FeEnt transport but could have been difficult to interpret during iron transport. With the loop conformational studies fully examined, residues in loops 4,

5, and 8 could be better candidates for energy transfer experiments if the Cys substituted mutants in FepA could bind and transport FeEnt similar to wild-type FepA.

A source of error may be assuming the external loops of FepA were 100% labeled with A546M. This assumption could have created issues when the distance between the dyes was calculated. If the fluorescent labeling of the external loops of FepA were not 100% covalently modified by A546M, the fluorescence intensity of the FM would be larger in the presence of the acceptor than the actual fluorescence intensity. FM would also label the free Cys residues that were not initially modified by A546M, therefore certain FepA proteins would have two FM dyes associated with it. This would make the previous energy transfer efficiency equation, $E = \left(1 - \frac{F_{DA}}{F_D}\right)$, irrelevant.

We determined the labeling efficiency of A546M by labeling the single extracellular Cys derivative of FepA S271C with FM after the acceptor dye, A546M (Fig. 29). This was analyzed by SDS-PAGE and an anti-FepA immunoblot. The fluorescence intensities in the gels and the amount of FepA present gave an idea of the labeling efficiency of A546M with FepA. The results indicated that the Cys mutant S271C in FepA was not 100% labeled by 5 μM A546M. The addition of 300 μM FM, appeared to show additional labeling of FepA S271C. A problem with this analysis was the limitation of the scan of fluorescence in the SDS-PAGE gel. The StormScanner excites at 450 nm and the emission is read at 520 nm, this

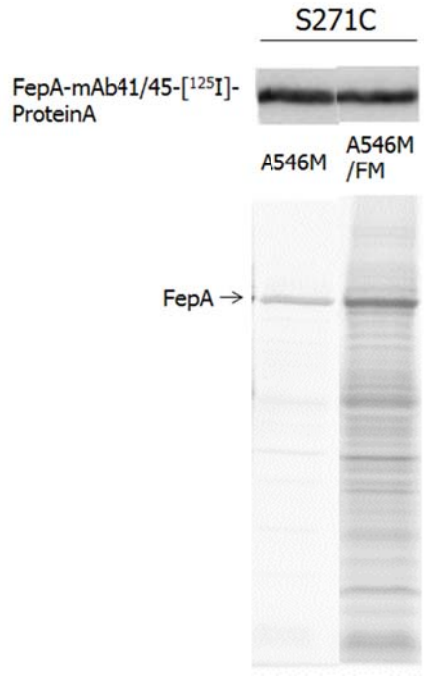

Figure 29. SDS-PAGE and immunoblot of Cys mutants S271C in FepA labeled with A546M with and without FM. To determine the labeling efficiency of A546M, we labeled the Cys substituted mutant S271C in FepA with 5 μM A546M. Then the samples were labeled with 300 μM FM. The cells were analyzed through SDS-PAGE and visualized by a StormScanner (**bottom lanes**). To compare the FepA expression in the samples, the proteins were transferred, incubated with anti-FepA mAb 41/45, [^{125}I]-protein A and scanned on a phosphorimager (**top lanes**). The fluorescence intensity of the double labeled single Cys mutant in FepA was greater than the single Cys mutant in FepA labeled with A546M alone.

is ideal for FM but is not ideal for A546M. This made the interpretation of the fraction of FepA labeled by A546M difficult.

Discussion

Several double Cys substituted mutants in FepA were constructed and we determined the effect of the Cys substitution(s) through siderophore nutrition assays, ^{59}FeEnt binding and ^{59}FeEnt transport determinations. We also conducted the ^{59}FeEnt binding and ^{59}FeEnt

transport assays with the Cys substituted mutants conjugated to the appropriate fluor to determine the effects of the dye. The Cys substituted derivatives of FepA were then subjected to fluorescence labeling with various concentrations of FM or A546M. Based on these results, we were able to determine which double Cys mutants in FepA were not ideal for FRET analysis.

We conducted emission scans with an excitation at 488 nm and excitation scans with an emission at 570 nm with the remaining suitable Cys substituted FepA derivatives to determine if energy transfer occurred between the two fluorophores. Initial studies indicated that energy transfer occurred between FM and A546M in the double Cys substituted mutant T30C/S271C in FepA. These results were not reproducible. To determine if energy transfer occurred during FeEnt transport through FepA, we conducted additional emission and excitation scans in the presence of FeEnt. The results indicated that energy transfer did not occur between the dyes this was unexpected based on previous experiments.

Based on the results that were accumulated, it indicated that further investigation was needed. For example, we could determine the fractional labeling of A546M. To determine the labeling efficiency of A546M, additional excitation and emission scans would have to be conducted. By labeling the same number of FepA Cys substituted mutant S271C cells with varying concentrations of A546M, a saturation curve which behaves under Michaelis-Menten conditions can determine a K_d value. Using this

value and the knowledge that A546M binds to FepA with a 1:1 ratio, the value of unlabeled FepA proteins can be determined. Once the labeling efficiency of A546M is determined, the fluorescence intensity with the emission at 520nm when excited at 488 nm of the double Cys mutant in FepA can be corrected for the presence of FepA proteins labeled with 2 FM dyes. Then an equation accounting for the fractional labeling with the acceptor dye, f_A, must be considered.

This could address the higher emissions at 520 nm of the samples containing both the donor and acceptor dyes. It would also help determine the appropriate concentration of A546M to use for maximal labeling efficiency by the acceptor dye. Aside from the fractional labeling, the orientation of the dipole of the dyes could also have contributed to the spectral results. The energy transfer efficiency is dependent, among others, upon the orientation factor, κ^2. In practice, it was assumed that the orientation factor is equal to 2/3 (62,66). This assumed the donor and the acceptor dye moved freely. This was probably not the case with FM conjugated to FepA. When FepA was covalently modified by FM, the dye was bound to the N-domain of FepA in an area surrounded by several other residues, which resulted in FM being more static than A546M. A546M modified a residue in FepA that was located on a mobile extracellular surface loop. Upgrades in instrumentation for the spectrofluorometer and phosphorimager have been made and this could

provide better analysis for the spectroscopic study of the FRET double Cys mutants in FepA.

Chapter 5: Determining conformational change in FepA during FeEnt uptake through disulfide bond formation

Background

A different approach to determining conformational change in FepA was taken by constructing several double Cys substituted mutants in FepA. The formation of disulfide bonds could provide information on the conformational motion within the N-domain of FepA and insight on FeEnt transport through FepA. The use of disulfide cross-linking to study transmembrane proteins have been applied before in several proteins, for example, LacY, ATP synthase, and G protein-coupled receptors (67-69). We constructed several double Cys substituted mutants in FepA to investigate the formation and hindrance of the disulfide cross-link in the absence and presence of FeEnt transport through FepA. Two classes of double Cys substituted mutants in FepA were engineered.

One class of double Cys mutant derivatives of FepA is referred to as N-terminus to N-terminus mutants, where both Cys mutants were engineered in the globular N-domain of FepA. The Cys residues are within cross-linking distance with the distance of the α-carbon atoms no greater than 6 Å (70,71). These double Cys mutant derivatives of FepA could form a cysteine bond and could affect the transport of FeEnt through FepA.

The second class of double Cys mutants in FepA is N-terminus to C-terminus mutants; one Cys substituted mutant in FepA is located in the N-domain and the other Cys mutant is located in the β-barrel of FepA with

the residue protruding into the OM channel. In this class of double Cys mutants the Cys residues are located far from one another and are unable to form a disulfide bond in native FepA, with the exception of one double Cys substitution in FepA. The N-terminus to C-terminus mutants were constructed to determine if the N-domain of FepA is dislodged into the periplasm during siderophore uptake. If the ball-and-chain model is supported, it is possible that the Cys mutant located in the N-domain would move into proximity of the remaining Cys mutant located on the C-domain and form a disulfide cross-link during FeEnt transport.

Experimental Procedures

Construction of double cysteine substitution mutants in FepA

We constructed seven double Cys substitutions in FepA. Four double Cys mutants in FepA were N-terminus to C-terminus mutants. With the exception of the double Cys mutant G54C/T585C in FepA, we engineered these based on the crystal structure of FepA and the likelihood they would interact if the globular N-domain were to exit the β-barrel. The other three double Cys mutants in FepA were N-terminus to N-terminus mutants. These were constructed based on the location of the residues and the likelihood they would form a disulfide bond in native FepA. The N-domain is comprised of a four stranded β-sheet and we engineered the double Cys substituted mutants in FepA on the β-sheet to restrict the mobility of the N-domain.

Once the single Cys substitutions were made in FepA, we constructed the double cysteine mutants by restriction fragment exchange with the endonucleases PstI and MluI. Cysteine substitutions were verified by DNA sequence analysis. Unless stated otherwise, all plasmids were harbored in OKN3 strains.

Siderophore accumulation

To measure the accumulation of ^{59}FeEnt in bacteria, we subcultured 1% stationary phase LB cultures into MOPS minimal media and allowed the bacteria to grow at 37°C until late log phase. Subcultures were conducted in the absence or presence of 1 mM β-mercaptoethanol. The assay was conducted at 37°C, which allowed ^{59}FeEnt binding and uptake. We took aliquots of the cells and placed the samples in a 37°C shaking water bath and ^{59}FeEnt was added to the cells to a final concentration of 5 μM ^{59}FeEnt. This concentration of ^{59}FeEnt saturated the cells and would not be depleted for several hours of transport even at a maximal rate ~ 100 pmol/min/10^9 cells (48). 100 μL aliquots of the cells were collected on nitrocellulose filters and rinsed with 0.9% LiCl after 5, 15, 25, 45, and 60 minutes. This was done in triplicate and the filters were counted to determine the accumulation of ^{59}FeEnt in the bacteria over a period of time. We measured the accumulation of ^{59}FeEnt by plotting the pmol ^{59}FeEnt/10^9 cells versus time.

Electrophoretic Mobility shift assays

Samples (1 x 10^8 cells) were analyzed using the SDS-PAGE system by Laemmli (72). We prepared the samples in the absence or presence of ~160 mM βME and boiled the samples for 5 minutes. Analysis with 50 μM N-ethylmaleimide (NEM) was also conducted, with the addition of the compound prior to the sample buffer. Two different SDS-PAGE gels were used to analyze the mobility shifts of the double Cys mutants in FepA. Samples were analyzed with a 10% SDS polyacrylamide gel (72) or with a modified protocol using 44% acrylamide and 0.3% bis-acrylamide in the resolving gel (73). The stacking gels in both analyses were 30% acrylamide and 0.8% bis-acrylamide. We electrophoresed the samples at room temperature for 2 hours and 15 minutes to increase resolution. The proteins were transferred to nitrocellulose paper. To determine the expression of FepA and the possible mobility shifts, we conducted immunoblots with anti-FepA mAb 41/45. After incubation with the primary antibody and washes with water or TBS and 0.05% tween 20, the blot was incubated with ^{125}I-protein A or alkaline phosphatase-conjugated goat anti-mouse IgG. The blots were visualized by a phosphorimager or colorimetrically with nitro blue tetrazolium and 5-bromo-4-chloro-3-indolyl phosphate, respectively.

Results

Double Cys substituted mutants in FepA

We constructed two classes of double Cys substituted mutants in FepA with varying distances between the Cys residues (Table 4). These classes were created to help determine the conformational change within the N-domain of FepA during FeEnt transport. Figure 30 shows the graphical representation of the N-terminus to N-terminus double Cys mutants in FepA. Figure 31 shows the graphical representations of the N-terminus to C-terminus double Cys substituted mutant in FepA.

Table 4.Two classes of double Cys substituted mutants in FepA

N-terminus to N-terminus	Distance between α-carbons (Å)
G27C/R126C	5.1
A33C/E120C	4.9
L125C/V141C	5.1
N-terminus to C-Terminus	
G54C/T585C	5.7
M77C/T457C	27.2
A138C/T427C	19.2
A138C/A445C	13.0

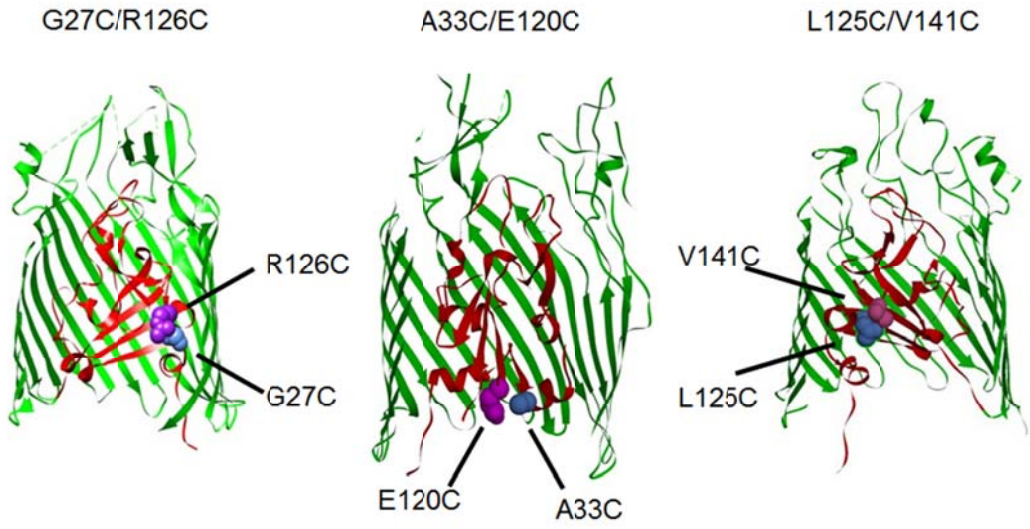

Figure 30. Graphical representation of N-terminus to N-terminus double Cys mutants in FepA.

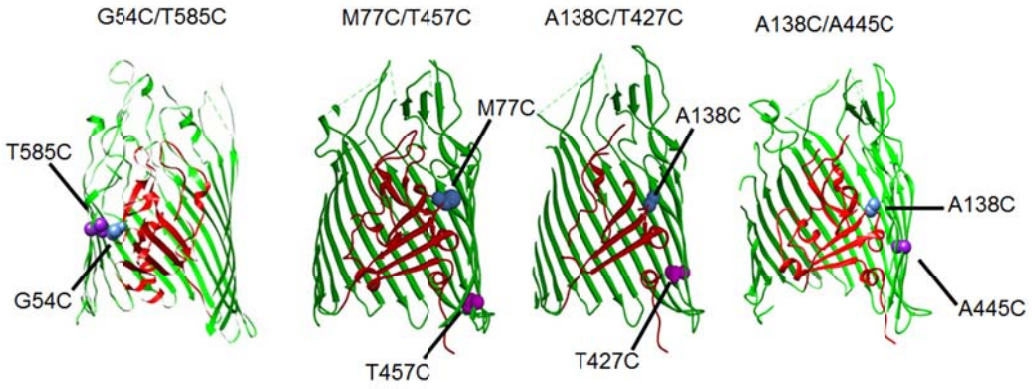

Figure 31. Graphical representation of N-terminus to C-terminus double Cys mutants in FepA.

To determine if the double Cys mutant derivatives of FepA showed functionality similar to wild-type FepA, we conducted siderophore nutrition tests (Fig. 32). If disulfide bonds were formed, it was possible the

functionality of FepA would be impaired and would not show positive siderophore nutrition test results (no halo). To determine the effects of a reducing environment, we conducted the siderophore nutrition test with various concentrations of βME present. In addition to assaying the double Cys mutants in FepA, the single Cys mutant derivatives of FepA were also subjected to siderophore nutrition tests (data not shown). All single Cys substituted mutants in FepA showed functionality similar to wild-type FepA.

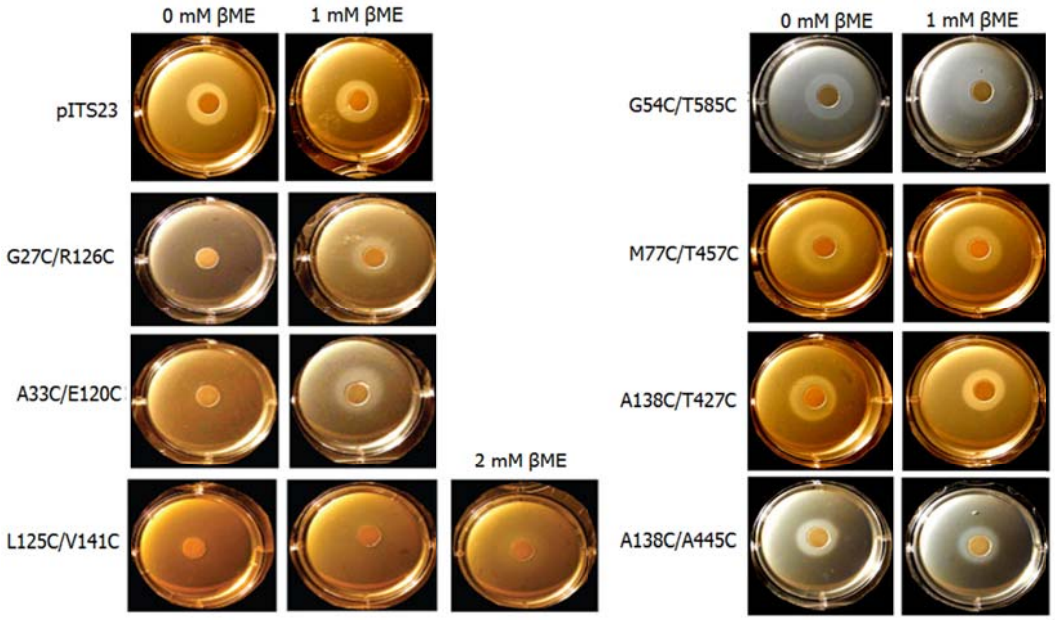

Figure 32. Siderophore nutrition tests of double Cys substituted mutants in FepA in the absence and presence of βME. Bacterial cultures were plated in LB media containing 233 μM bipyridyl. We placed a disc in the center of the agar and 0.5 nmol of FeEnt was added to the disc. The halo of the Cys substituted mutants were compared to wild-type pITS47. The N-terminus to C-terminus mutants were able to transfer FeEnt like wild-type FepA. The N-terminus to N-terminus mutants only showed positive siderophore nutrition results in the presence of the reducing agent βME.

The results of the siderophore nutrition test indicated that there was a distinct difference between the two classes of double Cys substituted mutants in FepA. The N-terminus to N-terminus mutants did not have bacterial growth halos in the absence of the reducing agent, βME. All of the N-terminus to N-terminus mutants were able to transport FeEnt in the presence of 1 mM β-mercaptoethanol, with the exception of the double Cys mutant L125C/V141C in FepA which a growth halo was only observed in the presence of 2 mM βME. This implied that these mutants were able to form a disulfide bond with the Cys substituted residues and this cross-link impaired the function of FepA during FeEnt transport. The N-terminus to C-terminus mutants showed similar FeEnt transport to the wild-type FepA in the siderophore nutrition tests in the absence and presence of the reducing agent.

We conducted a Colicin B (ColB) sensitivity assay with the N-terminus to N-terminus mutants in FepA (data not shown). Overnight cultures of the double Cys mutants in FepA with or without 1 mM βME were plated onto LB plates. A serial dilution of Colicin B was applied on to the plate and the titre was determined as the last ColB dilution able to clear the lawn of bacteria. The results indicated that all of the double Cys mutant derivatives of FepA were more resistant to ColB than the wild-type parent protein. In a reducing environment the double Cys mutants in FepA were twice as sensitive to ColB as in oxidative conditions. These results

suggested the formation of a disulfide bond within FepA also affected colicin sensitivity.

Effect of double Cys substitutions in FepA in FeEnt accumulation

To determine the effects of the double Cys mutants in FepA, we conducted a quantitative study in which the accumulation of the iron siderophore was measured over a period of time. All of the double Cys mutant derivatives of FepA were subcultured in the absence and presence of the reducing agent, β-mercaptoethanol. Similarly to the siderophore nutrition tests, if the double Cys mutants in FepA formed a disulfide bond with the Cys substituted mutants, which resulted in the hindrance of ^{59}FeEnt binding or transport, the accumulation of FeEnt would be less than wild-type FepA. The addition of βME during the subculture would reduce any possible thiol cross-links and the accumulation of ferric enterobactin should be similar to wild-type FepA.

Although the extent of accumulation differed between the three N-terminus to N-terminus mutants, the results indicated that FepA was impaired in the absence of a reducing agent and could not accumulate FeEnt like the wild-type parent protein. These results indicated that the double Cys mutants were able to form a disulfide bond in FepA. Fig. 33 showed the accumulation data collected from all three double Cys mutants in FepA. When the bacterial cultures were grown in a reducing environment, the accumulation of FeEnt in all of the N-terminus to N-terminus mutants in FepA was similar to the wild-type parent protein.

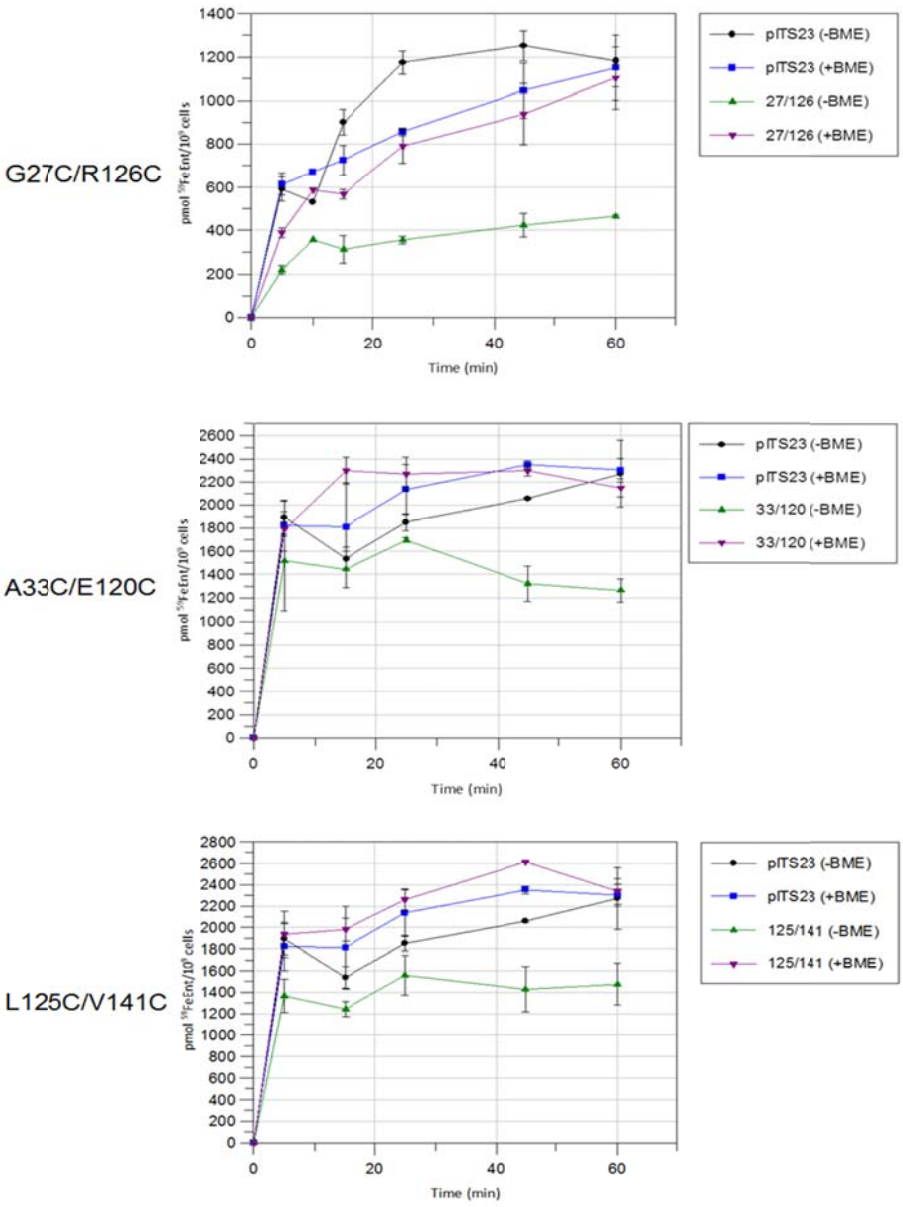

Figure 33. Accumulation of ^{59}FeEnt in the N-terminus to N-terminus mutants in FepA in the absence or presence of βME. We subcultured the double Cys substituted mutants G27C/R126C and A33C/E120C in FepA and wild-type FepA in MOPS minimal media (with or without 1 mM βME). The double Cys substituted mutant L125C/V141C in FepA and wild-type FepA were subcultured with or without 2 mM βME. After the addition of 5 μM ^{59}FeEnt, aliquots of the cells were collected, washed and counted at 5, 15, 25, 45, and 60 minutes. Data was collected in triplicate. The results shown were an average of several experiments.

The accumulation results observed in the N-terminus to C-terminus mutants differed from the N-terminus to N-terminus mutants in FepA. With the exception of the double Cys substituted mutant in FepA G54C/T585C, the double Cys mutants accumulated the iron complex similar to wild-type FepA. This was true in the absence and presence of βME. Figure 34 showed the results obtained for the remaining N-terminus to C-terminus mutants in FepA. The ability for the double Cys mutant derivatives of FepA to accumulate FeEnt suggested the Cys mutant residues never came into proximity with one another to form a disulfide bond. The double Cys substituted mutant G54C/T585C in FepA was unable to accumulate FeEnt similar to wild-type FepA in an oxidizing or reducing environment. The Cys residues in this double Cys mutant were within distance to form a disulfide bond. It was possible that a thiol cross-link was formed and βME could not reduce the disulfide bond that formed between G54C/T585C.

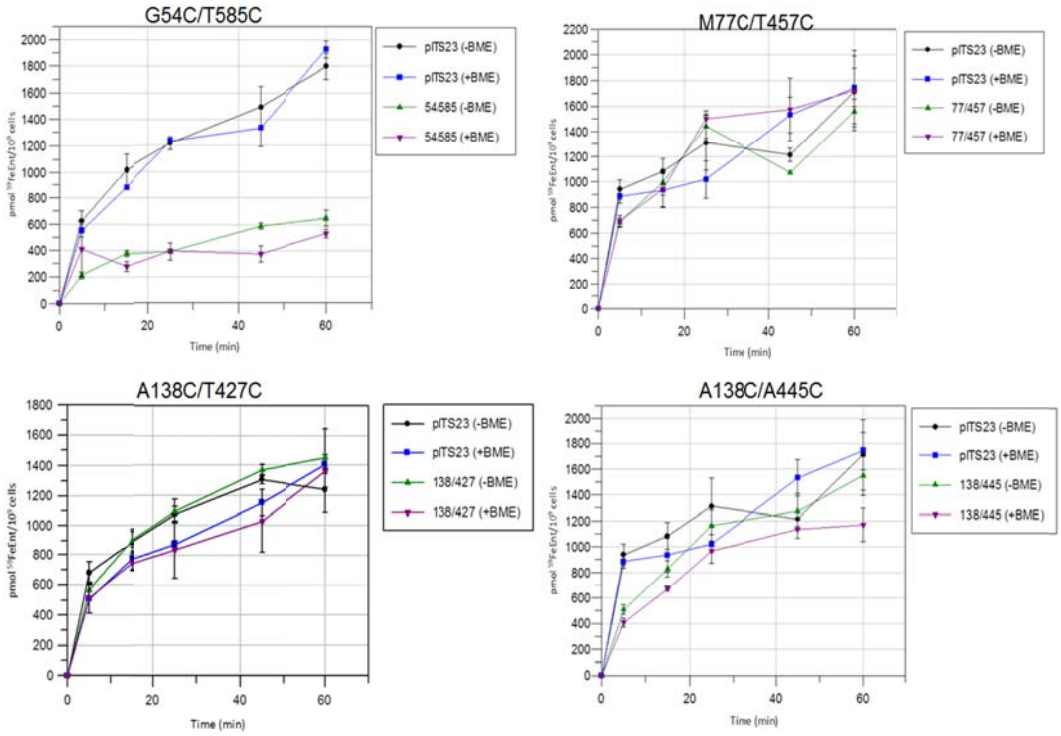

Figure 34. Accumulation of ^{59}FeEnt in the N-terminus to C-terminus mutant in FepA in the absence or presence of βME. We subcultured all of the N-terminus to C-terminus double Cys substituted mutants in FepA and wild-type FepA in MOPS minimal media (with and without 1 mM βME). After the addition of 5 μM ^{59}FeEnt, aliquots of the cells were collected, washed and counted at the various times. Data was collected in triplicate. The results shown were an average of a couple of experiments.

We compiled the ^{59}FeEnt accumulations results into a table (Table 5) to assess the effects of the double Cys substituted mutants in FepA during siderophore accumulation. The results in Table 5 were shown as the percentage of accumulation compared to wild-type FepA. The percentage of accumulation was determined by comparing the last accumulation measurement of the double Cys mutant in FepA (+/- βME) to wild-type FepA (+/- βME). The extent of ^{59}FeEnt accumulation provided

an indication of the functionality of the double Cys mutant in FepA compared to the wild-type pITS23.

The results indicated that a disulfide bond formed in the N-terminus to N-terminus double Cys mutants in FepA. The formation of the disulfide bond restrained the mobility of the N-domain within FepA and impaired the ability of FepA to accumulate FeEnt. The N-terminus to C-terminus double Cys mutants in FepA were all able to accumulate the siderophore similar to the wild-type FepA. This suggested that the globular N-domain of FepA did not exit the β-barrel of FepA. The only exception was G54C/T585C in FepA, which could form a disulfide bond and therefore hinder the transport of FeEnt through FepA.

Table 5. Accumulation results of double Cys mutants in FepA

Class of double Cys mutants in FepA	Accumulation compared to wild-type FepA	
N-terminus to N-terminus	**-βME**	**+ 1 mM βME**
G27C/R126C	40%	93%
A33C/E120C	56%	95%
L125C/V141C	47%	82%
N-terminus to C-Terminus	**-βME**	**+ 1 mM βME**
G54C/T585C	36%	30%
M77C/T457C	90%	100%
A138C/T427C	100%	100%
A138C/A445C	100%	98%

Effect of double Cys mutations in FepA during FeEnt binding and uptake

We conducted standard binding and uptake experiments on all of the double Cys mutant derivatives of FepA. Assays with the N-terminus to C-terminus double Cys mutants M77C/T457C, A138C/T427C, and A138C/A445C in FepA were initially conducted in the presence of copper/1,10-phenanthroline (CuP). The assays were conducted with millimolar concentrations of the oxidative catalyst and the results indicated that the high concentrations of CuP precipitated the ^{59}FeEnt, which made the results difficult to interpret (data not shown).

Initial binding assays with the double Cys mutants in FepA were conducted in the absence or presence of 1 mM βME. The *in vivo* binding capabilities of the double Cys mutants in FepA were compared to wild-type FepA by comparing the K_d values (23,26). Wild-type FepA has a K_d = 0.2 nM, in most of the double Cys mutants in FepA, the K_d values were at least an order of magnitude greater. This was because the binding results of the double Cys mutants in FepA did not display typical binding characteristics and were unable to be fitted properly to a single site saturation curve (Fig. 35).

The results seen in Fig. 35 were typical results seen in the other double Cys mutants in FepA (data not shown). This suggested that the formation of a disulfide bond may hinder the binding interactions between FepA and FeEnt.

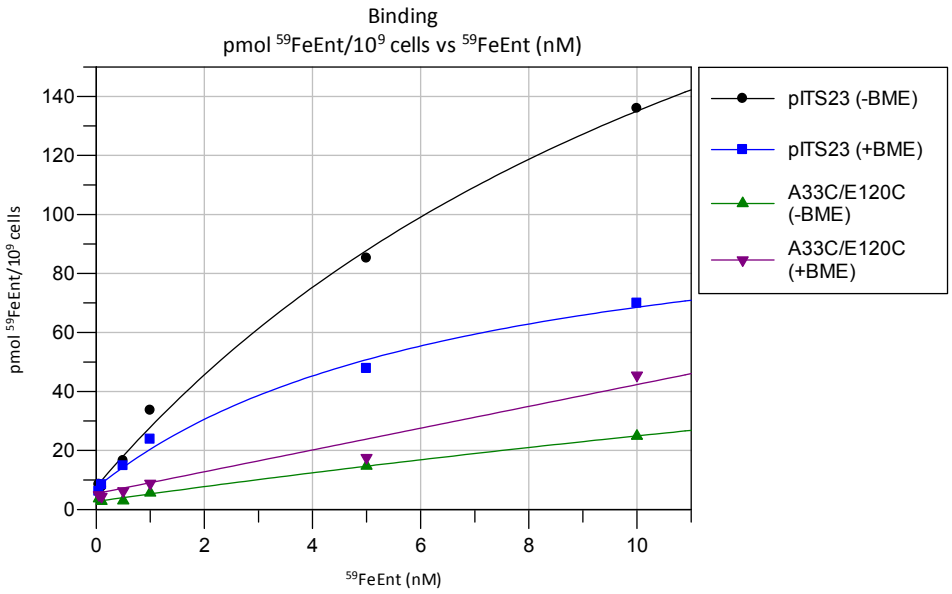

Figure 35. ^{59}FeEnt binding assay of the double Cys mutant A33C/E120C in FepA (+/- 1 mM βME). We subcultured overnight cultures into MOPS minimal media with or without 1 mM βME. The experiment was conducted on ice and ^{59}FeEnt was added at a series of concentrations: 0.05, 0.1, 0.5, 1.0, 5.0, and 10.0 nM. Aliquots of the cells were collected, washed, and counted. These measurements were done in triplicate. The double Cys mutant in FepA did not exhibit typical binding characteristics but did bind more ^{59}FeEnt in the presence of 1 mM βME.

We also conducted, standard ^{59}FeEnt uptake assays on the N-terminus to N-terminus mutants in FepA and it was determined the standard experimental conditions were not suitable for these mutants. Wild-type FepA had the expected V_{max} ~120 pmol ^{59}FeEnt(10^9 cells·min)$^{-1}$, but the double Cys mutants in FepA could not be fitted to the Michaelis-Menten equation. Standard uptake assays extrapolate the amount of FeEnt transport within 1 minute by measuring two separate time points: 5 seconds and 35 seconds. It could be possible that the latter time point was insufficient to measure FeEnt uptake through the double Cys mutant in FepA. Adjustments that were made to this assay included increasing the

last time measurement to 5 minutes and 5 seconds and increasing the concentration of ^{59}FeEnt.

Mobility shift

To determine the expression of FepA and the possible cross-link formation within FepA, we subjected the double Cys mutants in FepA to electrophoretic mobility shift assays (Fig. 36 and 37). The samples were analyzed using SDS-PAGE with a modified protocol using 44% acrylamide and 0.3% bis-acrylamide in the resolving gel (73). The stacking gels in both analyses were 30% acrylamide and 0.8% bis-acrylamide. Overnight cultures were subcultured in MOPS minimal media with or without 1 mM βME. The cells (1 x 10^8) were prepared in sample buffer also with or without 160 mM βME. To determine if the disulfide bond was formed after solubilizing FepA, we added N-ethylmaleimide (50 μM) in some of the samples. N-ethylmaleimide was added and the samples incubated at room temperature for 5 minutes before the addition of the sample buffer (+/-βME).

The results of the N-terminus to N-terminus mutants in FepA (Fig. 36) indicated that mutants G27C/S126C and A33C/E120C had a partial cross-link formation that led to increased elelctrophoretic mobility and a downward band shift. The band indicating increased mobility appeared in the absence and presence of N-ethylmaliemide but was not observed in the samples containing βME. A band similar to wild-type FepA was present, which indicated the fraction of the double Cys substituted mutant

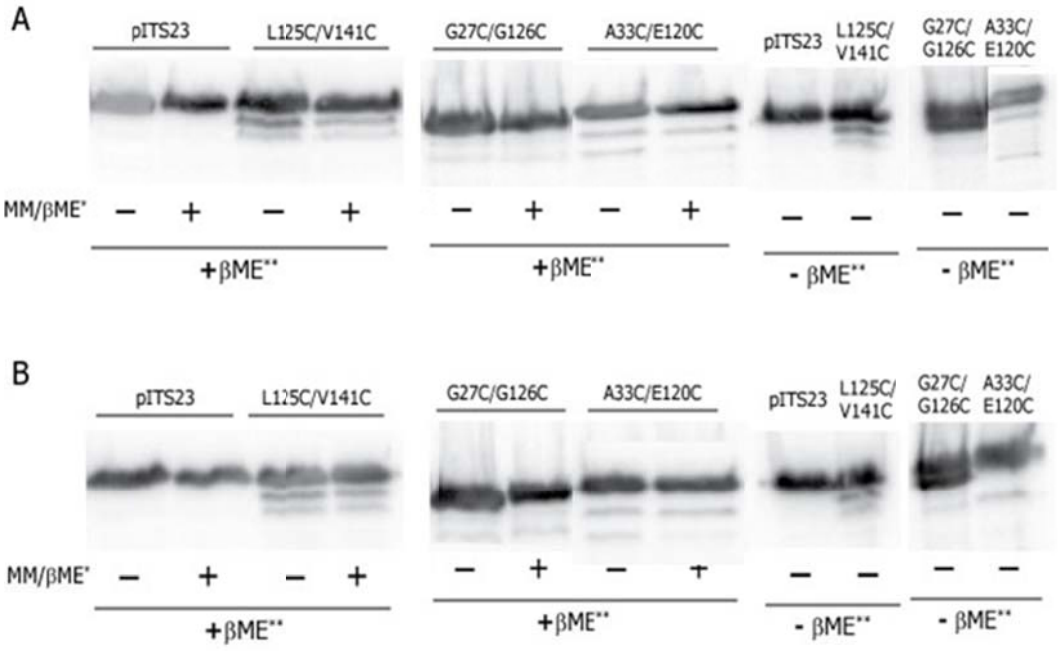

Figure 36. Anti-FepA immunoblots of N-terminus to N-terminus mutants in FepA. We subcultured overnight cultures in MOPS minimal media (MM*) in the absence (-) or presence (+) of 1 mM βME. Samples were then prepared in the absence (**panel A)** or presence (**panel B**) of 50 μM N-ethylmaleimide, then sample buffer (**) was added with (+) or without (-) ~160 mM βME.

in FepA that did not form a cross-link. This suggested that the disulfide bond formation occurred prior to solubilizing FepA. The double Cys mutant in FepA L125C/V141C did not show an additional FepA band that was not seen in the samples containing a reducing agent in the sample buffer.

The results of the N-terminus to C-terminus mutants in FepA varied from one another (Fig. 37). The double Cys mutants G54C/T585C and A138C/A445C both showed a partial disulfide bond formation that led to decreased elelctrophoretic mobility and an upward band shift. The band indicating decreased mobility appeared in the absence and presence of N-

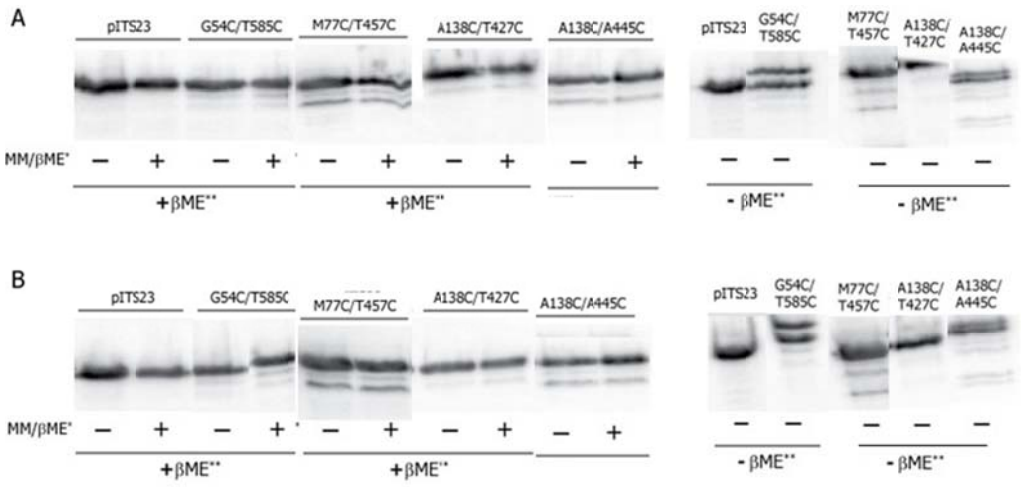

Figure 37. Anti-FepA immunoblots of N-terminus to C-terminus mutants in FepA. We subcultured overnight cultures in MOPS minimal media (MM*) in the absence (-) or presence (+) of 1 mM βME. Samples were then prepared in the absence (**panel A)** or presence (**panel B**) of 50 μM N-ethylmaleimide, then sample buffer (**) was added with (+) or without (-) ~160 mM βME.

ethylmaliemide but was not seen in the samples containing βME. This suggested that the cross-link occurred prior to solubilizing FepA.

Prior electrophoretic mobility shift assays were extensively conducted with the double Cys mutants A138C/T427C and M77C/T457C in FepA (Fig. 38 and 39). The samples were analyzed with a 10% SDS polyacrylamide gel. CuP was present in the samples to induce disulfide bond formation. We added FeEnt to the samples to determine the effect of FeEnt transport and cross-link formation. The samples were allowed to incubate at 37°C for 30 minutes or 1 hour. The results of both double Cys mutants indicated that a cross-link was formed that had decreased electrophoretic mobility and an upward band shift. This was not seen in the samples containing βME.

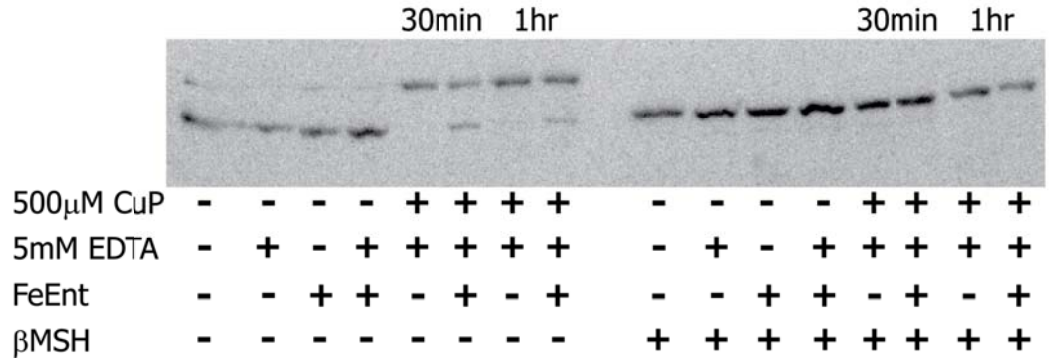

Figure 38. Anti-FepA immunoblot of the double Cys mutant A138C/T427C in FepA. We subcultured overnight cultures in MOPS minimal media. The samples were then treated with (+) or without (-) 500 μM CuP. To determine the effect of disulfide bond formation 5 nM FeEnt was absent (-) or present (+) during a 30 minute or 1 hour incubation period. 5 mM EDTA was absent (-) or present (+) to stop the reaction. The sample buffer was prepared with (+) or without (-) β-mercaptoethanol, βMSH. Experiment and figure prepared by Dr. Kyle Moore.

The results of the double Cys mutant A138C/T427C in FepA indicated that the cross-link formation was time dependent (Fig. 38) and increased during the 1 hour incubation period (additional incubation times were taken but the data is not shown). The addition of CuP also catalyzed cross-link formation between the Cys substituted mutants. If the N-domain of FepA exits the β-barrel of FepA during FeEnt transport, it would increase cross-link formation. This was not seen with the double Cys mutant A138C/T427C. The presence of FeEnt decreased the fraction of FepA that contained a disulfide bond between the Cys substituted residues. A band similar to wild-type FepA was present, which indicated the fraction of the double Cys substituted mutant in FepA that did not form a cross-link.

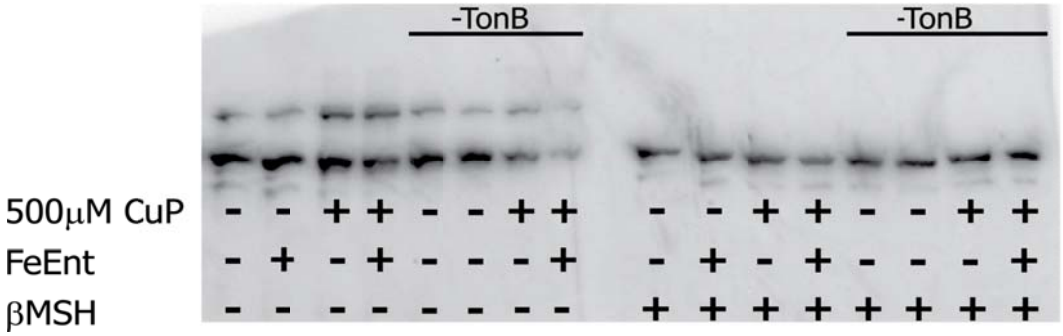

Figure 39. Anti-FepA immunoblot of the double Cys mutant M77C/T457C in FepA. We subcultured overnight cultures of pFepAM77C/T457C harbored in OKN3 (*ΔfepA*) or OKN13 (*ΔfepA*, *ΔtonB*) in MOPS minimal media. The samples were then treated with (+) or without (-) 500 μM CuP. To determine the effect of disulfide bond formation 5 nM FeEnt was absent (-) or present (+) during a 30 minute incubation period. Sample buffer was prepared with (+) or without (-) β-mercaptoethanol, βMSH. Experiment and figure prepared by Dr. Kyle Moore.

The results of the double Cys mutant M77C/T457C in FepA indicated that cross-link formation was effected in the absence of TonB (Fig. 39). In the presence of CuP the fraction of cross-linked Cys substituted mutant FepA increased. The absence or presence of FeEnt transport did not affect the cross-link formation.

Discussion

Table 6 summarized the results obtained throughout the study. The N-terminus to C-terminus mutants in FepA showed similar results to one another. The FeEnt accumulation assays and the siderophore nutrition tests showed no indication of a cross-link between the two Cys substituted residues in FepA. The electrophoretic mobility assays indicated that all of the double Cys mutants in FepA formed a disulfide bond. That was just a

qualitative assay and there were no quantitative results to determine the effects of the disulfide bond on FeEnt binding or transport.

Future investigations on the N-terminus to C-terminus mutants in FepA could involve the addition of EDTA during FeEnt binding and transport assays. This may help prevent FeEnt precipitation with CuP. It is also possible that aberrant disulfide bonds could form with the native cysteines present in FepA during FepA synthesis. One way to determine if the disulfide bond formation was genuine, we could engineer a Cys-less FepA derivative and construct the double Cys substituted mutants in the new construct.

The N-terminus to N-terminus double Cys mutants in FepA all formed a disulfide bond within the globular N-domain. This was supported by siderophore nutrition tests, FeEnt accumulation determinations, and mobility shift assays, with the exception of L125C/V141C, which showed no mobility shift. The study did show that the disulfide bond formation within the N-domain hindered FeEnt accumulation, which suggested the mobility of the N-domain is important during FeEnt transport through FepA.

Table 6. Summary of double Cys substituted mutants in FepA. *Results were seen in 10% SDS polyacrylamide gel and the samples were treated with CuP, N/A data not available

Double Cys Mutant in FepA	Siderophore Nutrition Test		Accumulation		Mobility Shift	
	-βME	+βME	-βME	+βME	-βME,-NEM	+βME,+NEM
N-Terminus to N-Terminus Mutants						
G27C/R126C	-	+	40%	93%	Gel shift down	Gel shift down
A33C/E120C	-	+	56%	95%	Gel shift down	Gel shift down
L125C/V141C	-	+	47%	82%	No gel shift down	No gel shift down
N-Terminus to C-Terminus Mutants	**-βME**	**+βME**	**-βME**	**+βME**	**-βME,-NEM**	**+βME, +NEM**
G54C/T585C	+	+	36%	30%	Gel shift up	Gel shift up
M77C/T457C	+	+	90%	100%	Gel shift up*	N/A*
A138C/T427C	+	+	100%	100%	Gel shift up*	N/A*
A138C/A445C	+	+	100%	98%	Gel shift up	Gel shift up

Chapter 6: Summary

The novel assay post-uptake binding allowed the direct measurement of FeEnt transport through the OM protein, FepA. Measurements with this assay revealed that all of the FepA proteins bound with the ligand were active and equivalent in FeEnt uptake. The activation energy of the FeEnt internalization through the OM was ~ 35 kcal/mol. Kinetic data suggested that ligand uptake through FepA was triphasic with the initial rate being the most rapid, the second rate had an intermediate rate, and the last rate was the slowest. Experiments indicated that FeEnt accumulation required the periplasmic binding protein and a complete inner membrane permease complex. After fluorescence and immunoprecipitation assays, FepA appeared to be actively transporting FeEnt but the accumulation of the ligand in the cytoplasm was impaired in the strain lacking the periplasmic binding protein. Experiments with strains lacking TolC indicated that it may be the source of FeEnt transport out of the cell.

After determining that all FepA bound to FeEnt actively transports FeEnt, we tried to determine the model of FeEnt transport through FepA using FRET analyses. We engineered several double Cys substituted mutants in FepA that were labeled with the donor and acceptor dyes, FM and A546M, respectively. By calculating the energy transfer between the dyes, we could determine the distance between the fluors. If we could determine the energy transfer between the dyes in the absence and

presence of FeEnt transport through FepA, we could determine the mechanism of FeEnt transport through FepA: ball-and-chain or transient pore model.

We determined the effect of the Cys substitution(s) through siderophore nutrition tests, ^{59}FeEnt binding, and ^{59}FeEnt transport assays. To determine the effect of the covalent modification by the fluorophores on the Cys substituted derivatives of FepA, we also conducted ^{59}FeEnt binding and ^{59}FeEnt transport assays after the cells were labeled with the appropriate fluor. We determined optimum labeling conditions for the Cys substituted derivatives of FepA for FRET analyses.

To determine if energy transfer between FM and A546M occurred, we ran excitation and emission scans of the single and double Cys substituted mutants in FepA after the cells were labeled with the appropriate fluor. We were unable to show reproducible results that indicated energy transfer between the dyes in the absence or presence of FeEnt transport through FepA. Two possible sources that could contribute to results indicating that energy transfer did not occur between the dyes could be the orientation of the dipoles of the dyes and if fractional labeling with A546M occurred. The former could be addressed by engineering double Cys substituted mutants in FepA in which the Cys substituted residues are mobile and are not confined. If fractional labeling of A546M occurred, the data collected from the emission scan would have to be adjusted to account for the fractional labeling.

In addition to FRET analyses, disulfide bond formation studies were conducted to determine the conformational change of the N-domain of FepA during FeEnt transport through FepA. We constructed two classes of double Cys mutants in FepA: N-terminus to N-terminus FepA mutants and N-terminus to C-terminus mutants in FepA. The Cys substituted mutants in FepA in the N-terminus to N-terminus mutants were designed so the Cys residues were within cross-linking distance.

To determine if the formation of a disulfide bond hindered the transport of FeEnt through FepA, we conducted assays in the absence and presence of FeEnt transport with these double Cys substituted mutants in FepA. Siderophore nutrition tests, FeEnt accumulation determinations, and mobility shift assays, with the exception of L125C/V141C, all indicated a formation of a disulfide bond within the globular N-domain of FepA. This cross-link hindered FeEnt accumulation through FepA. These results suggested that the mobility and flexibility of the N-domain of FepA was important during FepA mediated transport of FeEnt.

The second class of double Cys substituted mutants in FepA was N-terminus to C-terminus mutants. The Cys substituted residues in these mutants were engineered in which the residues could not form a disulfide bond in the native FepA and in the absence of FeEnt transport through FepA. If the N-domain of FepA is displaced into the periplasmic space, it is possible that the Cys residue in the N-domain could come in close

proximity of the Cys residue in the C-domain and form a disulfide bond. The FeEnt accumulation assays and the siderophore nutrition tests showed no indication of a cross-link formation between the two Cys substituted residues in FepA that hindered FeEnt transport through FepA. The electrophoretic mobility assays indicated that all of the double Cys mutants in FepA formed a disulfide cross-link. The mobility shift assays were just a qualitative assay and there were no quantitative results to determine the effects of the disulfide bond on FeEnt binding or transport.

References

1. Delcour, A. H. (2009) *Biochimica et biophysica acta* **1794**, 808-816

2. Hajjar, E., Mahendran, K. R., Kumar, A., Bessonov, A., Petrescu, M., Weingart, H., Ruggerone, P., Winterhalter, M., and Ceccarelli, M. (2010) *Biophysical journal* **98**, 569-575

3. Nikaido, H., and Pages, J. M. (2012) *FEMS microbiology reviews* **36**, 340-363

4. Brown, N. C., Eliasson, R., Reichard, P., and Thelander, L. (1968) *Biochemical and biophysical research communications* **30**, 522-527

5. Vernon, L. P. (1968) *Bacteriological reviews* **32**, 243-261

6. Yost, F. J., Jr., and Fridovich, I. (1973) *J Biol Chem* **248**, 4905-4908

7. Philpott, C. C., Klausner, R. D., and Rouault, T. A. (1994) *Proceedings of the National Academy of Sciences of the United States of America* **91**, 7321-7325

8. Weinberg, E. D. (1978) *Microbiological reviews* **42**, 45-66

9. Neilands, J. B. (1995) *J Biol Chem* **270**, 26723-26726

10. Klebba, P. E., McIntosh, M. A., and Neilands, J. B. (1982) *Journal of bacteriology* **149**, 880-888

11. Rogers, H. J. (1973) *Infection and immunity* **7**, 438-444

12. Cornelissen, C. N., and Sparling, P. F. (1994) *Mol Microbiol* **14**, 843-850

13. Raymond, K. N., Dertz, E. A., and Kim, S. S. (2003) *Proceedings of the National Academy of Sciences of the United States of America* **100**, 3584-3588. Epub 2003 Mar 24.

14. Hantke, K. (2001) *Current opinion in microbiology* **4**, 172-177

15. Miethke, M., and Marahiel, M. A. (2007) *Microbiology and molecular biology reviews : MMBR* **71**, 413-451

16. Pollack, J. R., and Neilands, J. B. (1970) *Biochemical and biophysical research communications* **38**, 989-992.

17. O'Brien, I. G., and Gibson, F. (1970) *Biochimica et biophysica acta* **215**, 393-402.

18. Loomis, L. a. R., Kenneth. (1990) *Inorganic Chemistry* **30**, 906-911

19. Tidmarsh, G. F., Klebba, P. E., and Rosenberg, L. T. (1983) *J Inorg Biochem* **18**, 161-168

20. Benson, S. A., and Decloux, A. (1985) *Journal of bacteriology* **161**, 361-367

21. Rutz, J. M., Liu, J., Lyons, J. A., Goranson, J., Armstrong, S. K., McIntosh, M. A., Feix, J. B., and Klebba, P. E. (1992) *Science* **258**, 471-475

22. Saier, M. H., Jr. (2000) *J Membr Biol* **175**, 165-180.

23. Newton, S. M., Igo, J. D., Scott, D. C., and Klebba, P. E. (1999) *Mol Microbiol* **32**, 1153-1165

24. Payne, M. A., Igo, J. D., Cao, Z., Foster, S. B., Newton, S. M., and Klebba, P. E. (1997) *J Biol Chem* **272**, 21950-21955

25. Buchanan, S. K., Smith, B. S., Venkatramani, L., Xia, D., Esser, L., Palnitkar, M., Chakraborty, R., van der Helm, D., and Deisenhofer, J. (1999) *Nat Struct Biol* **6**, 56-63

26. Cao, Z., Qi, Z., Sprencel, C., Newton, S. M., and Klebba, P. E. (2000) *Mol Microbiol* **37**, 1306-1317

27. Newton, S. M., Allen, J. S., Cao, Z., Qi, Z., Jiang, X., Sprencel, C., Igo, J. D., Foster, S. B., Payne, M. A., and Klebba, P. E. (1997) *Proceedings of the National Academy of Sciences of the United States of America* **94**, 4560-4565

28. Stephens, D. L., Choe, M. D., and Earhart, C. F. (1995) *Microbiology* **141**, 1647-1654

29. Krewulak, K. D., and Vogel, H. J. (2008) *Biochim Biophys Acta.* **1778**, 1781-1804. Epub 2007 Aug 19.

30. Chenault, S. S., and Earhart, C. F. (1991) *Mol Microbiol* **5**, 1405-1413

31. Shea, C. M., and McIntosh, M. A. (1991) *Mol Microbiol* **5**, 1415-1428

32. Langman, L., Young, I. G., Frost, G. E., Rosenberg, H., and Gibson, F. (1972) *Journal of bacteriology* **112**, 1142-1149

33. Klebba, P. E. (2005) *J. Bacteriol.* **187**

34. Braun, V. (1995) *FEMS microbiology reviews* **16**, 295-307

35. Bradbeer, C. (1993) *Journal of bacteriology* **175**, 3146-3150

36. Locher, K. P., Rees, B., Koebnik, R., Mitschler, A., Moulinier, L., Rosenbusch, J. P., and Moras, D. (1998) *Cell* **95**, 771-778

37. Larsen, R. A., Foster-Hartnett, D., McIntosh, M. A., and Postle, K. (1997) *Journal of bacteriology* **179**, 3213-3221

38. Ma, L., Kaserer, W., Annamalai, R., Scott, D. C., Jin, B., Jiang, X., Xiao, Q., Maymani, H., Massis, L. M., Ferreira, L. C., Newton, S. M., and Klebba, P. E. (2007) *J Biol Chem.* **282**, 397-406. Epub 2006 Oct 20.

39. Scott, D. C., Cao, Z., Qi, Z., Bauler, M., Igo, J. D., Newton, S. M., and Klebba, P. E. (2001) *J Biol Chem* **276**, 13025-13033.

40. Smallwood, C. R., Marco, A.G., Xiao, Q, Trinh, V., Newton, S.M.C. Klebba, P.E. (2009) *Mol. Microbiol.* **72**, 1365-1368

41. Newton, S. M., Trinh, V., Pi, H., and Klebba, P. E. (2010) *J Biol Chem* **285**, 17488-17497

42. Coleman, W. G., Jr., and Leive, L. (1979) *Journal of bacteriology* **139**, 899-910

43. Hashimoto-Gotoh, T., Franklin, F. C., Nordheim, A., and Timmis, K. N. (1981) *Gene* **16**, 227-235

44. Neidhardt, F. C., Bloch, P. L., and Smith, D. F. (1974) *Journal of bacteriology* **119**, 736-747

45. Luckey, M., Pollack, J. R., Wayne, R., Ames, B. N., and Neilands, J. B. (1972) *Journal of bacteriology* **111**, 731-738

46. Murphy, C. K., Kalve, V. I., and Klebba, P. E. (1990) *Journal of bacteriology* **172**, 2736-2746

47. Kaserer, W. A., Jiang, X., Xiao, Q., Scott, D. C., Bauler, M., Copeland, D., Newton, S. M., and Klebba, P. E. (2008) *J Bacteriol.* **190**, 4001-4016. Epub 2008 Apr 04.

48. Annamalai, R., Jin, B., Cao, Z., Newton, S. M., and Klebba, P. E. (2004) *Journal of bacteriology* **186**, 3578-3589.

49. Cao, Z., Warfel, P., Newton, S. M., and Klebba, P. E. (2003) *J Biol Chem* **278**, 1022-1028.

50. Hantke, K., and Braun, V. (1978) *Journal of bacteriology* **135**, 190-197

51. Schramm, E., Mende, J., Braun, V., and Kamp, R. M. (1987) *Journal of bacteriology* **169**, 3350-3357

52. Higgs, P. I., Larsen, R. A., and Postle, K. (2002) *Mol Microbiol.* **44**, 271-281.

53. Klebba, P. E. (2003) *Frontiers in Bioscience* **8:1422-1436**

54. Liu, J., Rutz, J. M., Feix, J. B., and Klebba, P. E. (1993) *Proceedings of the National Academy of Sciences of the United States of America* **90**, 10653-10657

55. Sprencel, C., Cao, Z., Qi, Z., Scott, D. C., Montague, M. A., Ivanoff, N., Xu, J., Raymond, K. M., Newton, S. M., and Klebba, P. E. (2000) *Journal of bacteriology* **182**, 5359-5364

56. Datsenko, K. A., and Wanner, B. L. (2000) *Proceedings of the National Academy of Sciences of the United States of America* **97**, 6640-6645.

57. Fairbanks, G., Steck, T. L., and Wallach, D. F. (1971) *Biochemistry* **10**, 2606-2617

58. Klebba, P. E., Benson, S. A., Bala, S., Abdullah, T., Reid, J., Singh, S. P., and Nikaido, H. (1990) *J Biol Chem* **265**, 6800-6810

59. Bleuel, C., Grosse, C., Taudte, N., Scherer, J., Wesenberg, D., Krauss, G. J., Nies, D. H., and Grass, G. (2005) *J Bacteriol.* **187**, 6701-6707.

60. Gutfreund, H. (1995) *Kinetics for the Life Sciences: Receptors, Transmitters and Catalysts*, Cambridge University Press, Cambridge, UK

61. Usher, K. C., Ozkan, E., Gardner, K. H., and Deisenhofer, J. (2001) *Proceedings of the National Academy of Sciences of the United States of America* **98**, 10676-10681.

62. Albani, J. R. (2007) *Principles and Applications of Fluorescence Spectroscopy*, Wiley-Blackwell

63. Kellogg, R. E. a. B., R. G. (1964) *The Journal of Chemical Physics* **41**, 3042-3045

64. Scott, D. C., Newton, S. M., and Klebba, P. E. (2002) *Journal of bacteriology* **184**, 4906-4911.

65. Smallwood, C. (2012) *In vivo* Fluorescence Characterization of the *Escherichia coli* Outer Membrane Protein FepA. in *Chemistry and Biochemistry*, University of Oklahoma, Norman, OK

66. Lakowicz, J. R. (1999) *Principles of Fluorescence Spectroscopy*, Second ed., Kluwer Academics/Plenum Publishers, New York

67. Zhou, Y., Madej, M. G., Guan, L., Nie, Y., and Kaback, H. R. (2011) *J Biol Chem* **286**, 30415-30422

68. Moore, K. J., and Fillingame, R. H. (2008) *J Biol Chem* **283**, 31726-31735

69. Zeng, F. Y., Hopp, A., Soldner, A., and Wess, J. (1999) *J Biol Chem* **274**, 16629-16640

70. Katz, B., and Kossiakof, A. (1986) *The Journal of Biological Chemistry* **261**, 15480-15485

71. Ozhogina, O. A., and Bominaar, E. L. (2009) *Journal of structural biology* **168**, 223-233

72. Laemmli, U. K. (1970) *Nature* **227**, 680-685

73. Lugtenberg, B., Meijers, J., Peters, R., van der Hoek, P., and van Alphen, L. (1975) *FEBS letters* **58**, 254-258